PLOS | ONE

RESEARCH ARTICLE

Identification of New Regions in HIV-1 gp120 Variable 2 and 3 Loops that Bind to α4β7 Integrin Receptor

Kristina K. Peachman[1,2], Nicos Karasavvas[3], Agnes-Laurence Chenine[1,2], Robert McLinden[1,2], Supachai Rerks-Ngarm[4], Kaewkungwal Jaranit[5], Sorachai Nitayaphan[6], Punnee Pitisuttithum[7], Sodsai Tovanabutra[1,2], Susan Zolla-Pazner[8¤a], Nelson L. Michael[1], Jerome H. Kim[1¤b], Carl R. Alving[1], Mangala Rao[1]*

1 U.S. Military HIV Research Program, Walter Reed Army Institute of Research, Silver Spring, MD, United States of America, **2** Henry M. Jackson Foundation for the Advancement of Military Medicine, Bethesda, MD, United States of America, **3** United States Army Medical Component, Armed Forces Research Institute of Medical Sciences, Bangkok, Thailand, **4** Ministry of Public Health, Bangkok, Thailand, **5** Data Management Unit, Mahidol University, Bangkok, Thailand, **6** Royal Thai Army, Armed Forces Research Institute of Medical Sciences, Bangkok, Thailand, **7** Vaccine Trials Center, Mahidol University, Bangkok, Thailand, **8** Veterans Administration New York Harbor Health Care System and NYU School of Medicine, New York, United States of America

¤a Current address: Division of Infectious Diseases, Icahn School of Medicine at Mount Sinai, New York, NY, United States of America
¤b Current address: International Vaccine Institute, Seoul, Republic of Korea
* mrao@hivresearch.org

OPEN ACCESS

Citation: Peachman KK, Karasavvas N, Chenine A-L, McLinden R, Rerks-Ngarm S, Jaranit K, et al. (2015) Identification of New Regions in HIV-1 gp120 Variable 2 and 3 Loops that Bind to α4β7 Integrin Receptor. PLoS ONE 10(12): e0143895. doi:10.1371/journal.pone.0143895

Editor: Aftab A. Ansari, Emory University School of Medicine, UNITED STATES

Received: September 11, 2015

Accepted: November 10, 2015

Published: December 1, 2015

Data Availability Statement: All relevant data are within the paper and its Supporting Information files. For Flow cytometry raw data files, please see the Supporting Information files.

Funding: This work was supported by a cooperative agreement (W81XWH-11-2-0174) between the Henry M. Jackson Foundation and the US Department of Defense. SZ-P is supported by a grant from the National Institutes of Allergy and Infectious Diseases (AI 100151) and by funds from the Department of Veterans Affairs. The funders had no role in study

Abstract

Background

The gut mucosal homing integrin receptor α4β7 present on activated $CD4^+$ T cells interacts with the HIV-1 gp120 second variable loop (V2). Case control analysis of the RV144 phase III vaccine trial demonstrated that plasma IgG binding antibodies specific to scaffolded proteins expressing the first and second variable regions (V1V2) of HIV envelope protein gp120 containing the α4β7 binding motif correlated inversely with risk of infection. Subsequently antibodies to the V3 region were also shown to correlate with protection. The integrin receptor α4β7 was shown to interact with the LDI/V motif on V2 loop but recent studies suggest that additional regions of V2 loop could interact with the α4β7. Thus, there may be several regions on the V2 and possibly V3 loops that may be involved in this binding. Using a cell line, that constitutively expressed α4β7 receptors but lacked CD4, we examined the contribution of V2 and V3 loops and the ability of V2 peptide-, V2 integrin-, V3-specific monoclonal antibodies (mAbs), and purified IgG from RV144 vaccinees to block the V2/V3-α4β7 interaction.

Results

We demonstrate that α4β7 on RPMI8866 cells bound specifically to its natural ligand mucosal addressin cell adhesion molecule-1 (MAdCAM-1) as well as to cyclic-V2 and cyclic-V3 peptides. This binding was inhibited by anti-α4β7-specific monoclonal antibody (mAb)

design, data collection and analysis, decision to publish, or preparation of the manuscript.

Competing Interests: The authors have declared that no competing interests exist.

ACT-1, mAbs specific to either V2 or V3 loops, and by purified primary virions or infectious molecular clones expressing envelopes from acute or chronic subtypes A, C, and CRF01_AE viruses. Plasma from HIV-1 infected Thai individuals as well as purified IgG from uninfected RV144 vaccinees inhibited (0–50%) the binding of V2 and V3 peptides to α4β7.

Conclusion

Our results indicate that in addition to the tripeptide LDI/V motif, other regions of the V2 and V3 loops of gp120 were involved in binding to α4β7 receptors and this interaction was blocked by anti-V2 peptide, anti-V2 integrin, and anti-V3 antibodies. The ability of purified IgG from some of the uninfected RV144 vaccinees to inhibit α4β7 raises the hypothesis that anti-V2 and anti-V3 antibodies may play a role in blocking the gp120-α4β7 interaction after vaccination and thus prevent HIV-1 acquisition.

Background

The HIV field has expended great efforts to determine the mechanism(s) of protection observed in the HIV-1 RV144 phase III clinical trial. Immune correlate analysis and subsequent secondary analysis showed that antibodies against the HIV-1 Env gp120 V1V2 region correlated inversely with the risk of infection [1], thus generating the hypothesis that these antibodies may have contributed to the protection. The antibodies targeted multiple binding epitopes in the V3 and V2 region including the mid-region of the V2 loop that contained conserved epitopes with the amino acid sequence KQKVHALFYKLDIVPI (HXB2 numbering sequence 169–184) [2–7]. This region included the integrin-binding motif LDI/V (residues 179–181) [8, 9].

Integrins are cell surface receptors that are involved in a number of functions including migration of cells to different tissues and cell adhesion [10, 11]. The α4β7 integrin receptor is a heterodimer consisting of an α4 subunit that can associate with either a β1 or a β7 subunit [12, 13]. Activated $\alpha_4\beta_7$ integrin on lymphocytes binds to its cognate ligand MAdCAM-1 expressed on endothelial cells leading to the adhesion, extravasation, and homing of these lymphocytes to the gut tissues. The importance of the gut homing receptor $\alpha_4\beta_7$ was further highlighted by the findings that it can also serve as a receptor for HIV-1 and SIV transmission leading to the up-regulation of LFA-1 and spread of HIV-1 from cell-to-cell through virological synapses [14, 15]. The $\alpha_4\beta_7$ integrin receptor on activated $CD4^+$ T cells provides a link between the earliest site of HIV-1 transmission, the mucosa, and the gut inductive sites where T cells are depleted during infection [16, 17].

We have recently shown in humanized DRAG mice ([Rag1KO.IL2RγcKO.NOD ("NRG") strain] with chimeric transgenes encoding for HLA-DR*0401 [HLA-DRA/HLA-DRB1*0401] fused to the I-Ed MHC- II molecule) [18] that after a vaginal HIV-1 challenge, the gut $\alpha_4\beta_7{}^+CD4^+$ T cells are infected with HIV-1 with a subsequent decrease in these cells during the course of HIV-1 infection [19]. It has been previously reported that in SIV infected rhesus macaques, the depletion of β7-expressing $CD4^+$T cells in the blood and in the intestine are comparable. Furthermore, a decrease in plasma and gastrointestinal viral loads was observed after administration of an $\alpha_4\beta_7$ monoclonal antibody prior to and during SIV infection [20]. A strong correlation between the frequencies of memory CD4 T cells expressing high levels of

α4β7 integrin and susceptibility to SIV rectal transmission has also been demonstrated [21]. The above findings therefore suggest that *in vivo*, α4β7 integrin may be playing an important role in SIV and HIV-1 transmission [22].

The interaction of HIV-1 envelope protein and the activated form of $\alpha_4\beta_7$ has been thought to be through a conserved tripeptide motif LDI(V) present at the tip of V2 loop of HIV-1 gp120 [8, 23]. It has been hypothesized that the extended form of α4β7 may facilitate this interaction, which might be instrumental for the "permanent" establishment of a HIV-1 positive state [8, 9, 23]. However, unlike CD4 and CCR5, which are required for viral entry, interaction with the $\alpha_4\beta_7$ receptor may not be essential for entry.

The mechanism of protection induced by anti-V2 antibodies and their influence on HIV-1 acquisition in the RV144 trial is still unclear. However, protection does not appear to be due to the neutralizing function of the antibodies [24]. Subsequently, two separate nonhuman primate studies demonstrated that antibodies directed against the V2 region reduced the acquisition of infection [25, 26]. It is possible that anti-V2 antibodies may function by either directly blocking or sterically hindering the $\alpha_4\beta_7$-gp120 interaction. However, the potential implications of gp120-V2 binding to $\alpha_4\beta_7$ integrin receptor in HIV transmission are still a topic of debate.

We examined the interactions between α4β7 integrin and either primary HIV-1 virions, or infectious molecular clones containing either acute or chronic envelopes, or peptides derived from the V2 and V3 regions of gp120 using RMPI8866 cells constitutively expressing the α4β7 integrin receptor. We also assessed the ability of V2- and V3-specific monoclonal antibodies (mAb) to block V2/V3 peptide-α4β7 integrin interaction. Finally, we tested the plasma of HIV-1 uninfected and infected individuals as well as IgG purified from RV144 vaccinees for the presence of α4β7 integrin blocking antibodies. Our data provide insights into new regions of HIV-1 gp120 that interact with α4β7 integrin molecule, which could have implications for future HIV-1 vaccine design.

Methods

Ethics statement, protocol authorization, and regulatory approval

RV144 (WRAIR Protocol #900): This clinical trial [27] protocol and all related documents were approved by the following independent Institutional Review Boards (IRBs): Division of Human Subject Protection, Walter Reed Army Institute of Research; Ethical Review Committee for Research in Human Subjects, Ministry of Public Health, Thailand. (http://clinicaltrials.gov/ct2/show/NCT00223080?term=RV144&rank=2;NCT00223080).

(WRAIR Protocol #1617): This protocol and all related documents were approved by the following independent Institutional Review Boards (IRBs): Division of Human Subject Protection, Walter Reed Army Institute of Research; Ethical Review Committee for Research in Human Subjects, Ministry of Public Health, Thailand. All volunteers provided written informed consent following discussion and counseling by the clinical study team prior to enrollment and before any trial related procedures were performed.

Cell line and reagents

The human B lymphoma cell line RPMI8866 that constitutively expresses α4β7 on its cell surface was purchased from Sigma-Aldrich. Cells were grown at a density of 3-9x10^5 cells/ml at 37°C and 5% CO_2 in the following media: RPMI 1640, 10% heat inactivated fetal bovine serum, 1% penicillin/streptomycin, and 1% glutamine (purchased from Quality Biologics Inc.; except for FBS which was purchased from Gemini Bio-Products). Peptides were synthesized with or without biotin at the amino terminus of the peptide by JPT Peptide Technologies (See Table 1 for sequences and lengths). Some of the peptides were cyclized by disulfide bond formation

Table 1. Amino Acid Sequences for V2 and V3 Peptides.

Cyclic or Linear peptide based on 92TH023 Strain	*HXB2 amino acid numbering*	*Amino Acid Sequence (Biotin-Ttds-peptide-NH_2) (Bold indicates changes from the original sequence)*
Cyclic V2 (42aa)	157–196	CSFNMTTELRDKKQKVHALFYKLDIVPIEDNTSSSEYRLINC
Cyclic V2 SMR	157–196	CSFNMTTELRDK**QVLFKDIHKIVKPLYA**EDNTSSSEYRLINC
Cyclic V2 SFL	157–196	**CENLTDKMFTSR**KQKVHALFYKLDIVPI**SESRLDETNYNISC**
Cyclic V2 SCR (42aa)	157–196	**CQLYSLFIRLTKVKITELMKYSNPVHSDKIREFNTDSNDAEC**
Linear V2 (42aa)	157–196	*XSFNMTTELRDKKQKVHALFYKLDIVPIEDNTSSSEYRLINX
Cyclic V3 (36aa)	295–331	CTRPSNNTRTSINIGPGQVFYRTGDIIGDIRKAYC
Cyclic peptide based on MN Strain	*HXB2 amino acid numbering*	*Amino Acid Sequence*
Cyclic V2 (40aa)	157–179	CSFNITTSIGDKMQKEYALLYKLDIEPIDNDSTSYRLISC
Cyclic V3 (35aa)	295–330	CTRPNYNKRKRIHIGPGRAFYTTKNIKGTIRQAHC
Cyclic peptide based on Acute C Strain C06980v0c22	*HXB2 amino acid numbering*	*Amino Acid Sequence*
Cyclic V2 (40aa)	157–179	CSFNITTELRDKRKKEHALFNNLDIVQLDGNSSLYRLINC
Cyclic V3 (35aa)	295–330	CTRPNNNTRKSIRIGPGQTFYATGDIIGDIRQAYC

*X = S-methyl Cysteine

doi:10.1371/journal.pone.0143895.t001

and the purity was determined to be greater than 90% by high pressure liquid chromatography and mass spectrometry. Streptavidin and AlamarBlue® were purchased from Invitrogen. MAdCAM-1 was purchased from R & D Systems. NeutrAvidin was purchased from Life Technologies Corp. The following reagents were obtained through the AIDS Research and Reference Reagent Program, Division of AIDS, NIAID, NIH: α4β7 monoclonal antibody, ACT-1, (cat#11718) from Dr. A. A. Ansari [20]. HIV-1_{IIIB} rgp120 (CHO expressed), ACT-1, a mouse monoclonal antibody that specifically binds to the α4β7 heterodimer including the active form, and pSG3Δenv were obtained through the AIDS Research and Reference Reagent Program, Division of AIDS, NIAID, NIH from Drs. John C. Kappes and Xiaoyun Wu. pSG3Δenv contains a four-nucleotide insertion mutation (CTAG) in envelope, leading to a translation stop codon after amino acid residue 142 [28, 29].

Expression of α4β7 on RPMI8866 cells

RPMI8866 cells (0.5 $x10^6$) were incubated for 30 minutes on ice with 10% normal goat sera in PBS to block the Fc receptors. Cells were suspended in cold FACS buffer (PBS-containing 0.5% BSA) and incubated at room temperature for 30 minutes with the mAb ACT-1 conjugated to APC (1 μg). Cells were washed twice with cold FACS buffer, fixed with 2% formaldehyde in PBS, and analyzed on a LSRII flow cytometer. The data was analyzed using FlowJo8.8.6 software (TreeStar Inc.).

Binding of gp120 and cyclic V2 peptide to α4β7 on RPMI8866 cells

RPMI8866 cells (1 $x10^6$) were suspended in cold FACS buffer (PBS-containing 0.5% BSA) and incubated at room temperature for 30 minutes with LIVE/DEAD® Fixable Dead Cell Stain (Life Technologies) as per the manufacturer's instruction. Cells were washed twice with cold FACS buffer before being incubated with 10% goat sera in PBS for 30 minutes on ice. All subsequent incubations were carried out for 30 minutes on ice. CHO- expressed HIV-1_{IIIB} rgp120 (2.5 μg) and biotinylated cyclic V2-TH023 peptide (1 μg and 5 μg) were incubated with

RPMI8866 cells. Following washing twice with cold FACS buffer, polyclonal mouse anti-gp145 (sera obtained from a mouse immunized three times with gp145 clade B protein encapsulated in liposomes containing monophosphoryl lipid A; unpublished data) was then added to cells previously incubated with gp120. Cells were washed and goat anti-mouse Texas Red (Thermo Fisher Scientific-Pierce) was added. Cyclic V2 TH023 (1 μg and 5 μg) fully scrambled V2 TH023 (SCR; 1 μg and 5 μg) treated samples were incubated with neutrAvidin-PE. Cells were washed twice with cold FACS buffer, fixed with 2% formaldehyde in PBS, and analyzed on a LSRII flow cytometer. The data was analyzed using FlowJo8.8.6 software (TreeStar Inc.). Peptide sequences are shown in Table 1.

RPMI8866 cell line dose curve

Serial two-fold dilutions of RMPI8866 cells in the log phase of growth starting at 4 x 10^5 cells were incubated in a 96-well plate with RMPI 1640 media (1% FBS, 1% pen/strep, 1% glutamine) and AlamarBlue® dye (10μL per well). The plate was incubated at 37°C (5% CO_2) for 8 hours. Fluorescence (Excitation 560 nm and Emission 590 nm) was measured at 1 hour intervals using a M2 plate reader (Molecular Devices). The relative fluorescence units were plotted against time in hours. Data points are the mean of 6 replicates.

Inhibition of binding of α4β7 on RPMI8866 cells to MAdCAM-1, V2 peptides, and V3 peptides

Triplicate wells of a 96-well U-bottom polystyrene plate (Immunlon) were coated overnight at 4°C with 100 μl of 2 μg/ml of MAdCAM-1 or Streptavidin diluted in 0.05 M bicarbonate buffer, pH 9.6. The streptavidin-coated plates were then incubated with biotinylated cyclic or linear V2 peptides or cyclic V3 peptides (5 μg/ml in bicarbonate buffer, See Table 1 for sequence data) for 1 hour at 37°C. The solution from the plates was discarded and the plates were then blocked with blocking buffer (25 mM TRIS, 2.7 mM potassium chloride, 150 mM sodium chloride, 0.5% casein, 4 mM manganese chloride, pH 7.2) for 1 hour at 37°C. The solution was discarded and the plates were incubated with sample buffer (25 mM TRIS, 2.7 mM potassium chloride, 150 mM sodium chloride, 4 mM manganese chloride, pH 7.2 containing 1% fetal bovine sera) for 45 minutes at 37°C. Plates were manually washed 4 times with blocking buffer followed by the addition of 2 x 10^5 RPMI8866 cells/well that had been pre-incubated for 45 minutes at 37°C with sample buffer, with sample buffer containing 0.5 μg/ml of mAb ACT-1 or as a control, normal mouse serum (1:100). Plates were then incubated at 37°C (5% CO_2) for 1 hour, washed 5 times with wash buffer followed by the addition of 100 μl of RPMI-1640 containing 1% FBS, pen/strep/glutamine. The adhered cells were detected by the addition of 10 μl of AlamarBlue® dye. Plates were incubated at 37°C (5% CO_2) for 8 hours. Fluorescence was measured at 2 hour intervals using a M2 plate reader. For each condition, a minimum of 2 to 12 independent experiments run in duplicate or triplicate was performed. The optimum amount of coating proteins/peptides and the amount of ACT-1 required to inhibit α4β7 on RPMI8866 cells was determined in separate experiments (data not shown). Peptide sequences are shown in Table 1.

Competitive inhibition of binding of α4β7 on RPMI8866 cells to MAdCAM-1 by cyclic V2 and V3 peptides, primary HIV-1, and Infectious Molecular Clones (IMCs)

96-well plates were coated with MAdCAM-1 as described above. RPMI8866 cells (2 X 10^6/ ml) were incubated with cyclic V2 or V3 MN, TH023, or acute subtype C (C-6980v0c22) peptides or with scrambled flanking region (SFL) or the mid region (SMR) TH023 V2 or with a

Table 2. Specificity of the Binding Inhibition.

Concentration	Mannose	p24	Ovalbumin
μg/ml	% Inhibition ± SD	% Inhibition ± SD	% Inhibition ± SD
0.2	6.7 ± 7.6	8.2 ± 5.6	7.2 ± 12.5
1.0	7.6 ± 8.8	14 ± 9.9	2.0 ± 3.5
5	16.3 ± 14.9	9.1 ± 8.7	13.6 ± 11.8
10*	0	0	18

No significant inhibition of α4β7 integrin binding to MAdCAM-1 in a competition assay by mannose, p24, and ovalbumin was observed. The data represent the average of 3–7 experiments performed in triplicate.

*The data represent the average of triplicate determinations from a single experiment for this concentration.

doi:10.1371/journal.pone.0143895.t002

completely scrambled (SCR) TH023 peptide (10 μg/ml) for 45 minutes at 37°C before being added in triplicate to the MAdCAM-1 coated plates for 1 hour at 37°C. In concurrent experiments, RMI8866 cells were incubated with purified primary HIV-1 (0.75 ng to 6 ng/well p24) subtype B (SF162, US-1, JRFL), subtype CRF01_AE viruses (92TH023), IMCs (0.75 ng to 1000 ng/well p24 in each case) containing acute or chronic envelopes (Acute CRF01_AE (703357) [GenBank:JN944658], C (C-6980v0c22) [GenBank:HM215344], A(851891); Chronic CRF01_AE (CM235.2) [AF259954.1], C (ET02220LucR) [U46016]) [30–32] or with pSG3Δenv. pSG3Δenv contained a four-nucleotide insertion mutation (CTAG) in Env, leading to a translation stop codon after amino acid residue 142. The pSG3Δenv clone is routinely used for generating Env pseudotyped infectious virions.

Viruses were tested in triplicate in two independent experiments. In additional experiments, mannose, HIV-1 p24, and ovalbumin (0.2–10 μg/ml) were used in the competition assay as nonspecific protein controls (data in Table 2; 3–7 experiments performed in triplicate), whereas, an anti-RSV mAb, Synagis® was used as a nonspecific antibody control. Synagis® was incubated for 45 minutes with either MAdCAM-1 or with RPMI8866 cells and then placed in the assay system. The remainder of the assay was similar to that described above. Significance was determined by paired Student's t test.

Inhibition of binding of α4β7 on RPMI8866 cells to MAdCAM-1 by V2 or V3 specific mAbs, plasma from HIV-1 uninfected and infected individuals, or purified IgG from vaccinated individuals

Streptavidin-coated plates were incubated with biotinylated cyclic V2 TH023 peptide (5 μg/ml in bicarbonate buffer as described above) for 1 hour at 37°C. RPMI8866 cells (2 X 10^6/ml) were incubated with V2-specific mAbs (CH58, CH59), V2i mAbs (830A, 2158), V3 specific mAbs (2219, 2557) or with a non-V2-specific mAb CH54 (5–50μg/ml), plasma from HIV-1 uninfected or naturally infected individuals (WRAIR protocol #1617), or with purified IgG (WRAIR Protocol #900) (10 μg/ml) from RV144 pre and post-vaccinated (6 month) individuals for 45 minutes at 37°C before being added in triplicate to the peptide coated plates for 1 hour at 37°C. The rest of assay is similar to that described in detail above. CH58, CH59, and CH54 are human monoclonal antibodies isolated from RV144 vaccinees [33]. 830A, 2158, 2219, and mAb 2557 are also human mAbs. The mean of triplicates is shown in the graphs.

Results

Expression of α4β7 on RPMI8866 cells and binding to HIV-gp120 V2 peptide

The human B-cell lymphoma cell line, RPMI8866, has been reported to stably express integrin α4β7 on its cell surface [34]. In order to determine the percentage of RPMI8866 cells that constitutively express α4β7, cells were incubated with APC-labeled ACT-1 antibody and then analyzed on a LSRII flow cytometer (Fig 1A; S1 Data, S2 Data and S3 Data). ACT-1 is a conformational-specific anti-α4β7 mouse mAb, which binds the α4β7 heterodimer including the active form. Over 99% of RPMI8866 cells bound ACT-1, demonstrating that these cells constitutively express the functional form of α4β7. Each cell expressed approximately 100,000 α4β7 receptors on its cell surface (data not shown). It has been demonstrated that the V2 loop of HIV-1 envelope protein gp120 binds to the activated form of α4β7 on CD4+ T lymphocytes [8]. To determine if α4β7 integrin on RMPI8866 cells could bind to gp120 envelope protein and also to the V2 loop, cells were incubated with CHO-expressed subtype B gp120 (Fig 1B; S4 Data and S5 Data), biotinylated cyclic V2 92TH023 peptide (subtype CRF01_AE; henceforth referred to as TH023, see Table 1 for sequence), or biotinylated cyclic fully scrambled (SCR) V2 TH023 peptide (Fig 1C; S6 Data, S7 Data, S8 Data, S9 Data and S10 Data) followed by the addition of polyclonal mouse anti-gp145 sera and Texas red-labeled goat anti-mouse antibody (Fig 1B; S5 Data) or neutrAvidin-PE (Fig 1C; S6 Data, S7 Data, S9 Data and S10 Data) and then analyzed by flow cytometry. Both gp120 protein (Fig 1B) and cyclic V2 TH023 peptide (Fig 1C) bound to α4β7 expressed on the surface of RPMI8866 cells, while the SCR peptide (S6 Data and S9 Data) showed similar binding as the unstained cells (Fig 1C; S8 Data).

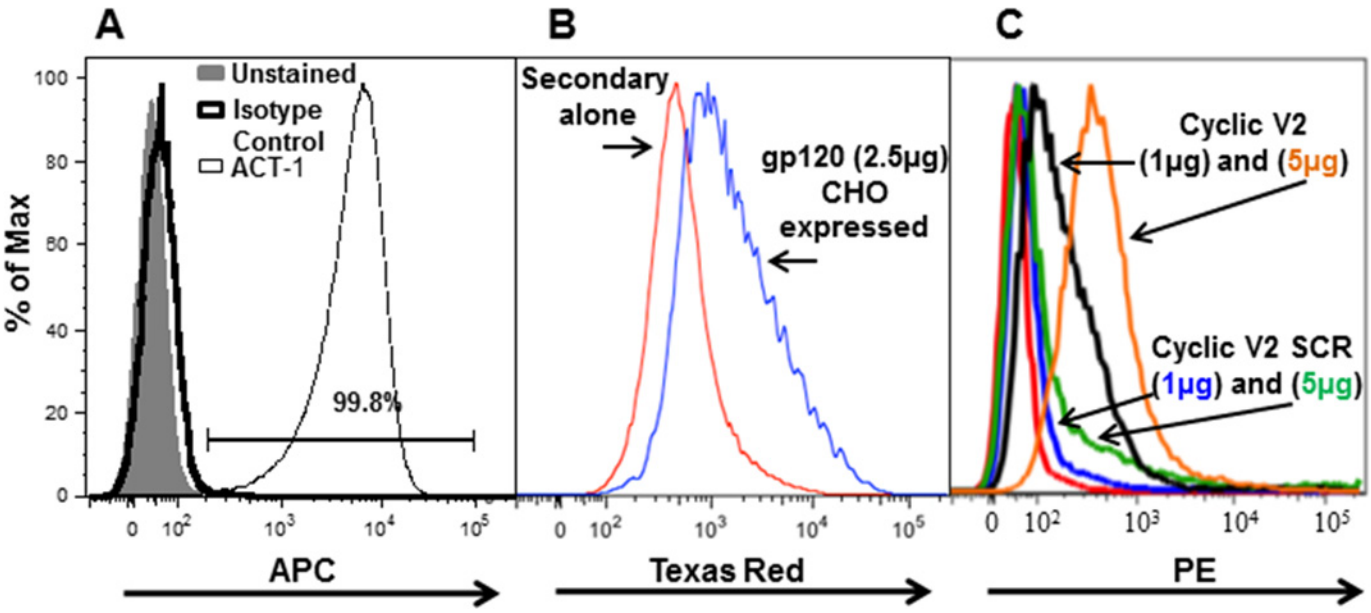

Fig 1. Binding of mAb ACT-1, HIV-1 gp120, and cyclic V2 peptides to RMPI8866 cells. (A) RPMI8866 cells (0.5 x10^6) were incubated with 1 μg APC labeled ACT-1 (α4β7 specific antibody). Antibody binding was measured by flow cytometry and is presented as a histogram. Over 99% of the RPMI8866 cells expressed α4β7 integrin. Unstained cells (grey shading) and isotype control antibody (solid line) were used as controls. **(A and C)** Histograms show the binding of CHO-expressed HIV-1 gp120 (2.5 μg, blue line panel **B),** biotin labeled cyclic V2 TH023 peptide (1μg and 5 μg; black and orange lines, respectively; panel **C**), and biotin labeled cyclic V2 TH023 -fully scrambled peptide (SCR; 1 μg and 5 μg; blue line and green line; panel **C**) to RMPI8866 cells. Polyclonal mouse anti-gp145 antibody followed by goat anti-mouse-Texas Red was used to visualize the gp120 protein binding while the V2 peptides were visualized with neutrAvidin-PE. Cells treated with only anti-mouse-Texas Red (red line, panel **B**) and unstained cells (red line, panel **C**) were used as controls in addition to the fully scrambled V2 peptide (blue and green line, panel **C**). Representative histograms are shown for panels **A**, **B**, and **C** (n = 2).

doi:10.1371/journal.pone.0143895.g001

Inhibition of binding of α4β7 to MAdCAM-1 by mAb ACT-1

In order to utilize this cell line to detect interactions between proteins, peptides, viruses, and antibodies to α4β7, we standardized an *in vitro* assay system for quantitating bound cells using AlamarBlue®, a water-soluble, nontoxic, and permeable reagent that contains resazurin, an oxidation-reduction indicator, which is reduced by metabolically active cells to resorufin, a highly fluorescent red compound. The magnitude of fluorescence signal quantified by a fluorometer is proportional to the number of live bound cells. Varying numbers of RMPI8866 cells in 2-fold dilutions starting at 400,000 cells/ well were plated in RMPI-1640 -phenol free media containing 1% FBS, pen/strep, and glutamine. AlamarBlue® dye was added and fluorescence was measured at 1 hour intervals for 8 hours. As shown in Fig 2A, the fluorescence was dose-dependent. As the cell number increased, there was a proportional increase in the level of fluorescence due to increased reduction of resazurin. Depending on the metabolic state of the cell, the fluorescence can range from 9,000 to 12,000 units at the 8 hour time point. Fluorescence units below 1,000 was considered as background fluorescence. For the three highest numbers of cells (100,000, 200,000, and 400,000), the fluorescence reached a plateau before the 8 hour time point. We chose 200,000 cells/well for all further experiments unless mentioned otherwise.

In order to determine if MAdCAM-1, the natural ligand of α4β7 integrin, could bind to α4β7 on the surface of RPMI8866 cells, 96-well plates were coated with MAdCAM-1. After blocking the wells, RPMI8866 cells pre-incubated in the absence (closed circles) or presence of mAb ACT-1 (open circles) were added to the wells, washed, and the binding of α4β7 on RPMI8866 cells to MAdCAM-1 was detected by the fluorescence of the added AlamarBlue® dye (Fig 2B, schematic diagram and graphs). Pre-incubation of RPMI8866 cells with ACT-1 mAb would block the interaction of α4β7 with MAdCAM-1, thus reducing the number of RPMI8866 cells that would adhere to the plate. This would result in a reduced fluorescence signal. The data are plotted as fluorescence units over time and represent the average of 6–12 experiments done in duplicate or triplicate ± SEM. In the absence of mAb ACT-1 (closed circles), approximately 12,000 fluorescence units were obtained by 8 hours representing 100% binding, while a decrease in the fluorescence units in the presence of mAb ACT-1 indicated an inhibition of binding of α4β7 integrin to its ligand. Based on this, the percent inhibition was calculated. ACT-1 inhibited the binding of α4β7 to MAdCAM-1 by 74%, while the control (normal mouse sera at a dilution of 1:100) did not inhibit the binding, thus showing the specificity of inhibition (data not shown).

Inhibition of binding of α4β7 to MAdCAM-1 by HIV-1

In order to demonstrate that HIV-1 envelope protein on the surface of virions is capable of binding α4β7 and thus inhibiting the binding of α4β7 to MAdCAM-1, varying amounts (based on p24 concentrations) of purified primary viruses including subtype B (SF162, US-1, JRFL), subtype CRF01_AE (92TH023; Fig 3A), full-length infectious molecular clones (IMCs) from acute viruses from subtypes CRF01_AE, C, and A (Fig 3B), and chronic IMC viruses from subtypes CRF01_AE and C (Fig 3C) were pre-incubated with RPMI8866 cells and then added to MAdCAM-1-coated plates (Fig 3). As a control, pSG3Δenv IMC with a frame shift in the envelope region was used in the assay at concentrations of p24 ranging from 0 to 500ng. The average inhibition of binding of α4β7 to MAdCAM-1 by pSG3Δenv IMC virus was 10 ± 2%. This cut off value is represented as a dotted line in all of the panels of Fig 3. As shown in Fig 3A (panel 1), a significant dose-dependent inhibition of binding of α4β7 on RPMI8866 cells to MAdCAM-1 was observed in the presence of SF162 virions ($p = 0.001$ and $p = 0.01$ comparing 6 ng/well vs 0.75 ng/well and 3 ng/well, respectively), demonstrating that SF162 virions bind to

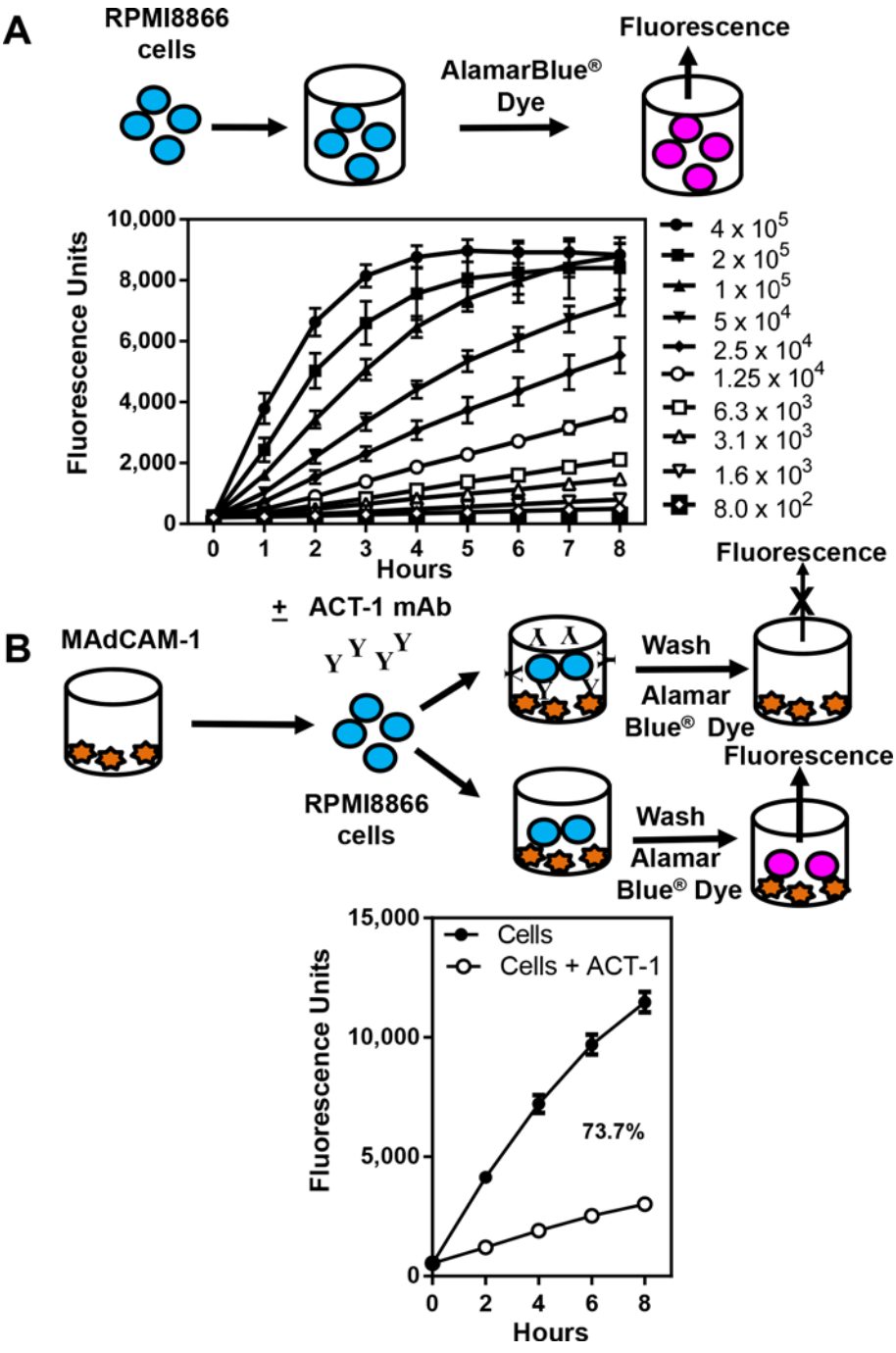

Fig 2. RPMI8866 cell titration curves and inhibition of binding of α4β7 integrin receptor to MAdCAM-1. (**A**) The top of the Fig shows a schematic representation of the experiment. Varying numbers of RPMI8866 cells in media were added to 96-well U bottom plates followed by the addition of AlamarBlue® dye. Cell numbers ranged from 800–400,000 cells per well. The plate was incubated at 37°C in a CO_2 incubator. Fluorescence was measured for 8 hours at 1 hour intervals using a M2 plate reader (excitation 560 nm; emission 590 nm). The data are plotted as relative fluorescence units as a function of time. The average ± S.D. of six replicates for each time point are shown. (**B**) Schematic of the assay set up. RMPI8866 cells were incubated with media only (solid circles) or with ACT-1 (0.5 μg/well; open circles, left panel) and then added to MAdCAM-1 (natural ligand of α4β7 integrin; 0.2 μg/well) coated plates. The plates were washed and 100 μl of media and 10 μl of AlamarBlue® dye were added to each well. Fluorescence was measured immediately after the addition of the dye (time 0) and then at 2 hours intervals for 8 hours. The percent inhibition at the 8 hour time point is shown. The data are plotted as relative fluorescence units as a function of time and represent the average ± SEM of 12 experiments done in triplicate.

doi:10.1371/journal.pone.0143895.g002

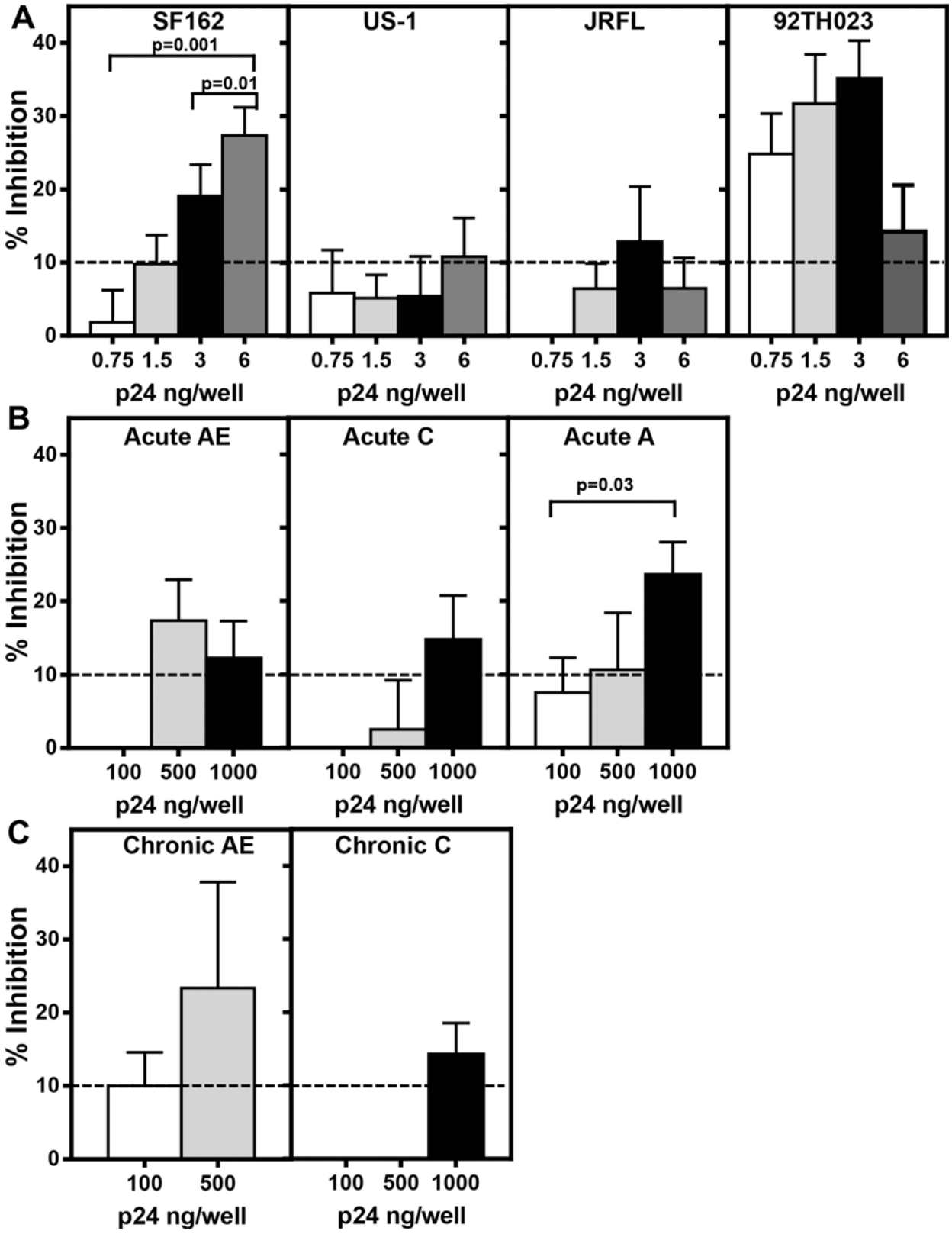

Fig 3. Inhibition of α4β7 integrin binding by primary virus and IMC's containing acute or chronic envelopes. Increasing concentrations of **(A)** purified primary subtype B viruses, SF162 (left panel), US-1 (second panel), JRFL (third panel) and subtype CRF01_AE (92TH023; right panel), **(B)** IMCs with acute

envelopes (subtype CRF01_AE left panel, subtype C center panel, and subtype A right panel), or **(C)** IMCs with chronic envelopes (subtype CRF01_AE left panel and subtype C right panel) were pre-incubated with RPMI8866 cells before being added to MAdCAM-1 coated plates. Primary viruses, except US-1 and JRFL, and IMCs inhibited the binding of α4β7 on RMPI8866 cells to MAdCAM-1 at one or more concentrations of the virus tested. The average percent inhibition of α4β7 integrin binding ± SEM as a function of p24 concentration is plotted for two independent experiments assayed in duplicate or triplicate for each virus or IMC. The dotted line represents the cut off value as determined by using a pSG3Δenv IMC with a frame shift in the envelope region. Significance was determined by paired Student's t test.

doi:10.1371/journal.pone.0143895.g003

α4β7 on RPMI8866 cells and block its interaction with MAdCAM-1. A dose-dependent increase in inhibition of binding was also observed with 92TH023 (Fig 3A, right panel) with inhibition (approximately 25–35%) observed at a p24 concentration of 0.75–3 ng /well. In contrast, a dose-dependent inhibition of α4β7 binding by US-1 and JRFL was not observed (Fig 3A, second and third panels). The acute and chronic IMCs showed varying degrees of inhibition at the concentrations of the virus tested, whereas the chronic subtype C IMC virus inhibited the binding only at the highest concentration of the virus tested. Compared to the primary viruses, a much higher concentration of IMCs was required to inhibit α4β7 binding to MAdCAM-1. These results show that the envelope protein present on the surface of the virions is capable of binding α4β7 on RPMI8866 cells and thus prevent the binding to MAdCAM-1 to varying degrees.

Binding of α4β7 integrin to HIV-1 envelope gp120 V2 and V3 peptides

It has been previously reported that the binding of α4β7 integrin receptor to HIV-1 envelope protein is through the V2 region [8]. Using our assay, we examined whether cyclic and linear V2 peptides could bind to α4β7 on RMPI8866 cells and whether the binding could be inhibited by ACT-1. The sequences of the gp120 V2 peptides (TH023, MN, and Acute C (C06980v0c22)) used are presented in Table 1. A schematic of the assay design is shown in Fig 4A. Plates, 96-well U-bottom, were coated with streptavidin followed by biotinylated linear or cyclic V2 peptides. After blocking the wells, RPMI8866 cells pre-incubated in the absence (closed circles) or presence of mAb ACT-1 (open circles) were added to the wells, washed, and the binding of α4β7 on RPMI8866 cells to the V2 peptides was measured by the fluorescence of resorufin (Fig 4B). Depending on the ability of α4β7 on RPMI8866 cells to bind the various peptides tested, the fluorescence varied from 3,000 to 9,000 units. The data are plotted as fluorescence units over time and represent the average of 6–12 experiments done in duplicate or triplicate ± SEM. The percent inhibition was calculated as described above and ranged from 63–72% for the various peptides tested (Fig 4B). Similar degrees of inhibition were obtained with both linear and cyclic TH023 peptides. The control normal mouse sera in 4 independent experiments done in triplicate showed an inhibition of 2 ±1% (data not shown).

Similar experiments were performed with biotinylated cyclic V3 peptides derived from subtypes CRF01_AE (TH023), B (MN), and acute subtype C (C06980v0c22) viruses. V3 peptides bound α4β7 integrin on RPMI8866 cells (Fig 4C), which could be specifically inhibited by ACT-1 (68–76% inhibition). The above data demonstrate that synthetic linear and cyclic V2 and cyclic V3 peptides derived from subtypes CRF01_AE, B, and acute C bind to α4β7 integrin on RPMI8866 cells and can be readily measured using our assay system. The binding is specific and can be inhibited by ACT-1.

Competition assay using V2 and V3 peptides and characterization of the V2 peptide region that interacts with α4β7 integrin

The schematic for the peptide competition assay is shown in Fig 5A. RPMI8866 cells were pre-incubated with varying concentrations (1 or 10 μg/ml) of cyclic V2 and V3 (TH023 or MN)

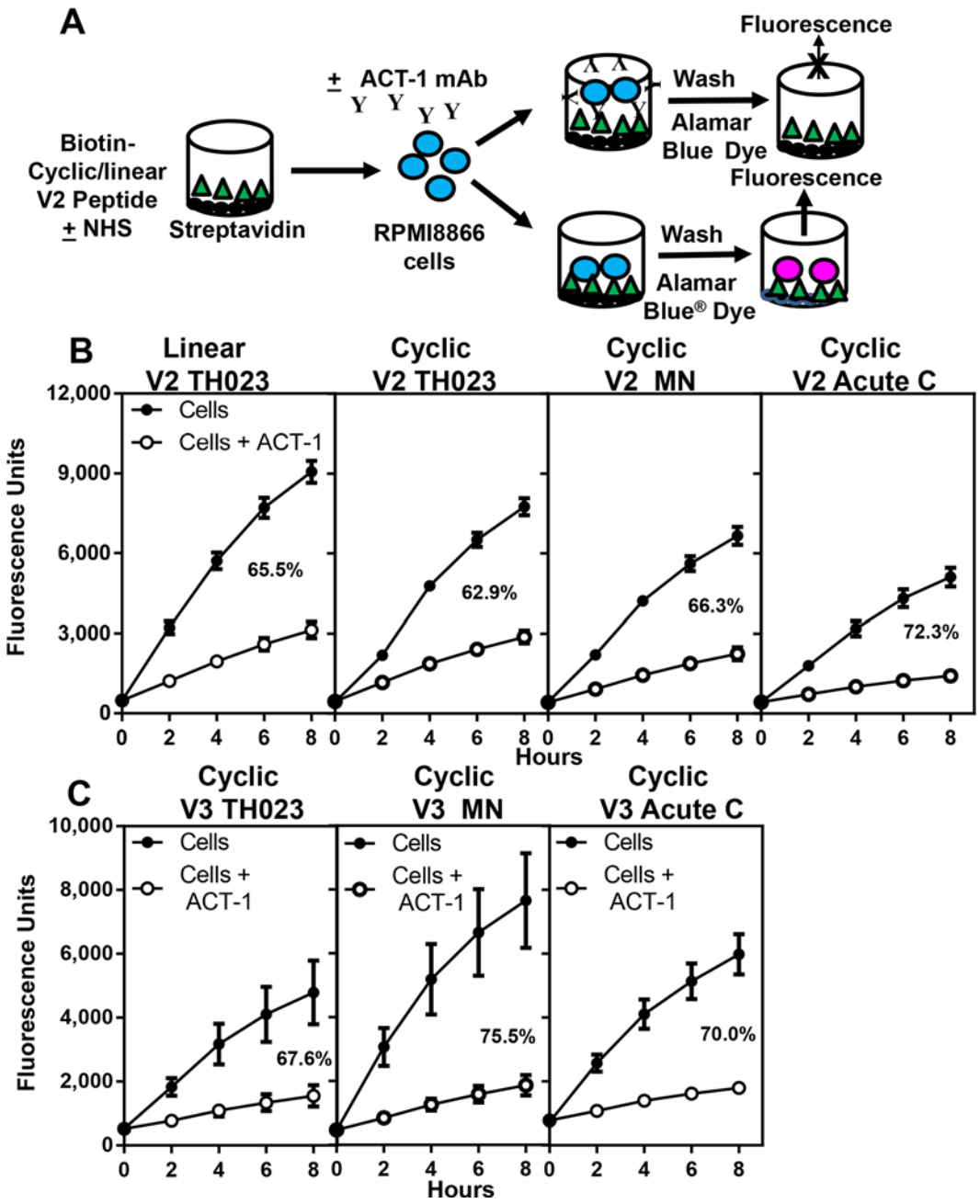

Fig 4. Binding of α4β7 integrin receptor to cyclic and linear V2 peptides. (A) Schematic of the assay set up. **(B and C)** RMPI8866 cells were incubated with media (solid circles), ACT-1 (open circles) and then added to (**B**) linear (left panel), cyclic V2 peptides (TH023, MN, and acute C, second, third and right panels, respectively), or (**C**) cyclic V3 peptides (TH023, left panel, MN, middle panel, and acute C, right panel) coated plates respectively. The plates were washed and 100 μl of media and 10 μl of AlamarBlue® dye was added to each well. Fluorescence was measured immediately after the addition of the dye (time 0) and then at 2 hour intervals for 8 hours. The percent inhibition at the 8 hour time point is shown in each panel. The data are plotted as relative fluorescence units as a function of time and represent the average ± SEM of 3 to12 experiments done in duplicate or triplicate.

doi:10.1371/journal.pone.0143895.g004

before being added to MAdCAM-1-coated plates (Fig 5B). A dose-dependent inhibition of α4β7 integrin binding to MAdCAM-1 was observed with all four of the peptides with approximately 80–90% inhibition at the 10 μg/ml concentration. In order to rule out the possibility of non-specific binding of proteins or sugars to RPMI8866 cells, HIV-1 p24, ovalbumin, or

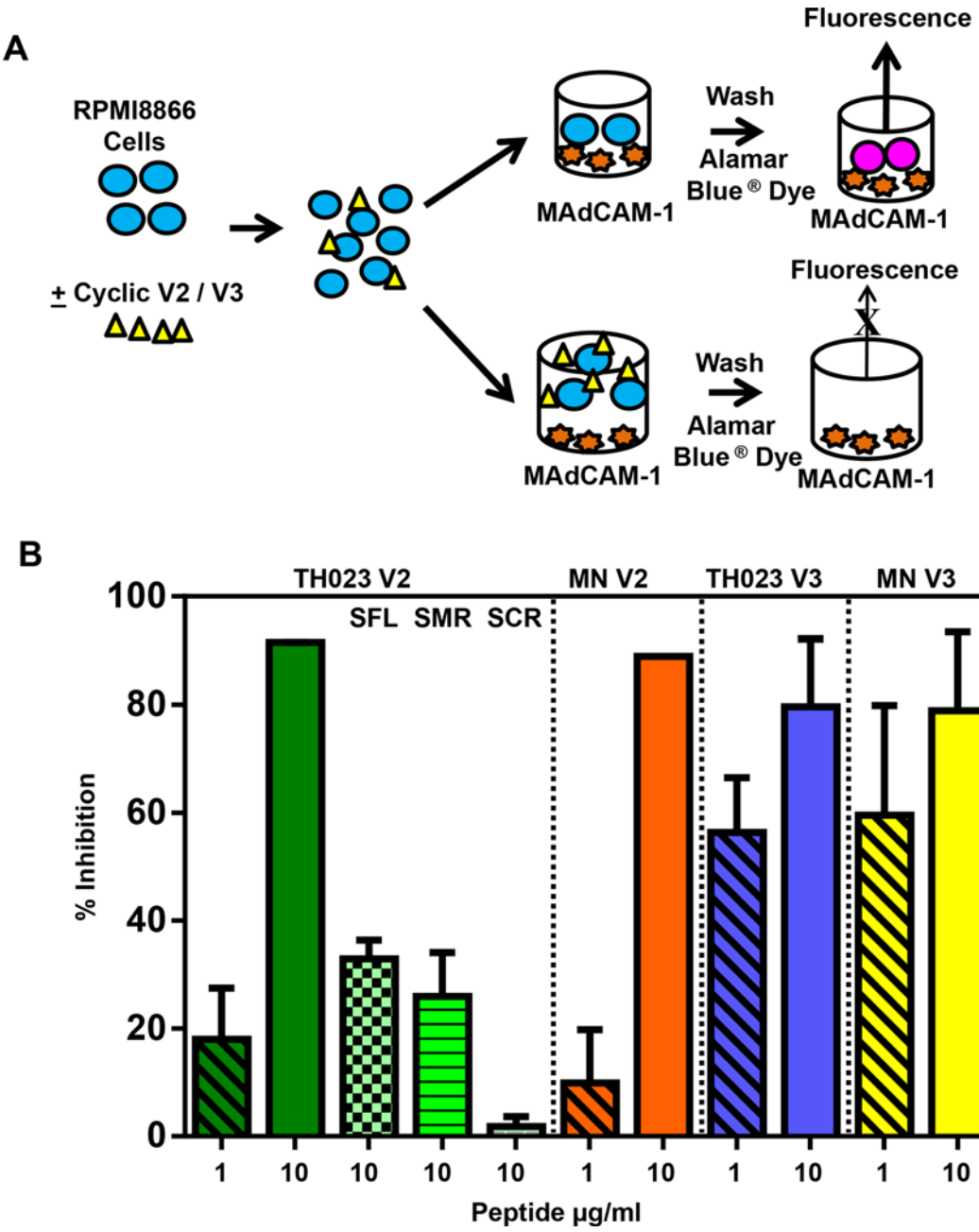

Fig 5. Competition of cyclic V2 and V3 peptides with MAdCAM-1 for binding to α4β7 integrin receptor. (A) Schematic of the assay set up. **(B)** Cyclic V2 and V3 peptides compete with MAdCAM-1 for binding to the integrin receptor. RPMI8866 cells were incubated with 1 (diagonal bars) or 10 µg/ml of cyclic V2 TH023 (solid green bar), cyclic V2 MN peptides (solid orange bar), cyclic V3 TH023 (solid blue bar) or cyclic V3 MN (solid yellow bar), respectively before being added to MAdCAM-1 coated plates. Data points represent the average fluorescence units ± SEM of 2–4 experiments done in triplicate. In separate experiments, RPMI8866 cells were also incubated with 10 µg/ml of cyclic V2 TH023 scrambled flank regions (SFL, green checkerboard bar), scrambled mid region (SMR, green horizontal bar) or fully scrambled (SCR, green brick bar) peptides respectively before being added to MAdCAM-1 coated plates. The binding of α4β7 on RPMI8866 cells to the fully scrambled peptide was lower than the binding to the scrambled mid region or the scrambled flank region. The data is shown as the average % inhibition ± SEM of 2 independent experiments done in triplicate.

doi:10.1371/journal.pone.0143895.g005

mannose, were added as controls in the competition assay (Table 2). Ovalbumin, p24, and mannose showed no significant inhibition.

In the RV144 immune correlates study, the vaccine-induced responses targeted multiple binding epitopes in the mid region of the V2 loop (aa 169–184) that contained the integrin-binding motif LDI/V, which is also the motif present in MAdCAM-1. The vaccine-induced responses were associated with a decreased proportion of infecting viruses carrying residue K169 and an increased proportion of infecting viruses carrying I181 [35]. Therefore, biotinylated cyclic V2 peptides with scrambled flanking regions (SFL), scrambled mid-region (SMR), or fully scrambled mid and flanking regions (SCR), were synthesized (Table 1) [6]. RMPI8866 cells were incubated with each of these peptides to map the V2 loop regions that bind to the integrin receptor and thus inhibit the binding to MAdCAM-1 (Fig 5B). In contrast to the 80–90% inhibition of binding of MAdCAM-1 to α4β7 on RPMI8866 cells observed with cyclic V2 and V3 TH023 peptides, 30–38% inhibition was obtained with SFL (green checkerboard bar) and SMR (green horizontal bar) V2 peptides (Fig 5B, first panel). The V2 SFL peptide retains the K169 and the I181 residues, whereas the V2 SMR peptide has K169Q and I181L. The fully scrambled V2 peptide, SCR showed less than 2% inhibition demonstrating that the V2 flanking and mid regions contribute to integrin receptor binding.

Inhibition of binding of α4β7 to V2- and V3-peptides by specific mAbs

Since both cyclic V2 and V3 peptides bound α4β7 on RPMI8866 cells and inhibited the binding of α4β7 to its natural ligand MAdCAM-1, we next examined if human mAbs specific for V2 and V3 regions would prevent the binding of the peptides to α4β7 on RPMI8866 cells. Two V2-specific mAbs CH58 and CH59, which bind to the mid region of the V2 loop and are CRF01-AE specific, were used along with a control mAb (CH54), which does not bind to the V2 or V3 region. These 3 mAbs were isolated from RV144 vaccinees [33]. In addition, two V2 integrin binding (V2i) human mAbs, 830A and 2158 [36], which bind to gp120 and V1V2 fusion proteins [33], but not to linear V2 peptides were also tested [37]. All of these mAbs were incubated with cyclic V2 TH023 peptide-coated plates (Fig 6A, 6B, 6C and 6D) followed by the addition of RMPI8866 cells. The CH58 and CH59 mAbs inhibited the binding of RMPI8866 cells by 33% and 42%, respectively (Fig 6A and 6B). The control mAb CH54 (closed triangles) as expected did not inhibit the binding (Fig 6B). Of the two human V2i mAbs tested, 2158 inhibited the binding of cyclic V2 peptide to α4β7 on RPMI8866 cells by 24% (Fig 6D), while 830A did not inhibit the binding (Fig 6C). These 5 mAbs were also tested with cyclic V2 MN peptide (Fig 6E, 6F, 6G and 6H). CH58, CH59, and CH54 did not inhibit the binding of α4β7 on RPMI8866 cells to V2 MN peptide even at concentrations of 50 μg/ml (Fig 6E and 6F), thus demonstrating the specificity of inhibition obtained with the TH023 peptide, as the epitope that the mAbs CH58 and CH59 recognize are not present in the subtype B MN V2 cyclic peptide. Again, only mAb 2158 at a concentration of 5 μg/ml inhibited the binding of MN peptide to α4β7 on RPMI8866 cells by 26% (Fig 6H). As a control, Synagis®, a mAb against Respiratory Syncytial Virus (RSV) was added to MAdCAM-1 coated plates followed by the addition of RPMI8866 cells (Fig 6I) or RPMI8866 cells were preincubated with Synagis® (Fig 6J) and then added to MAdCAM-1 coated plates. In both cases, Synagis® did not inhibit the α4β7 binding thus demonstrating the specificity of the assay and that the mAb was not nonspecifically adhering to the surface of RPMI8866 cells.

Human V3-specific mAbs (2219 and 2557) were incubated with either cyclic V3 TH023 (Fig 7A and 7B) or V3 MN peptide-coated plates (Fig 7C and 7D). Although mAbs 2219 and 2557 did not inhibit the binding of α4β7 on RPMI8866 cells to cyclic V3 TH023 peptide, they did inhibit the binding to cyclic V3 MN peptide. MAb 2219 showed a dose-dependent inhibition of 45% and 65% at 5 μg/ml and 10 μg/ml of antibody respectively (Fig 7C), while mAb 2557 showed a slightly lower inhibition of 18% and 33% (Fig 7D). These results are in

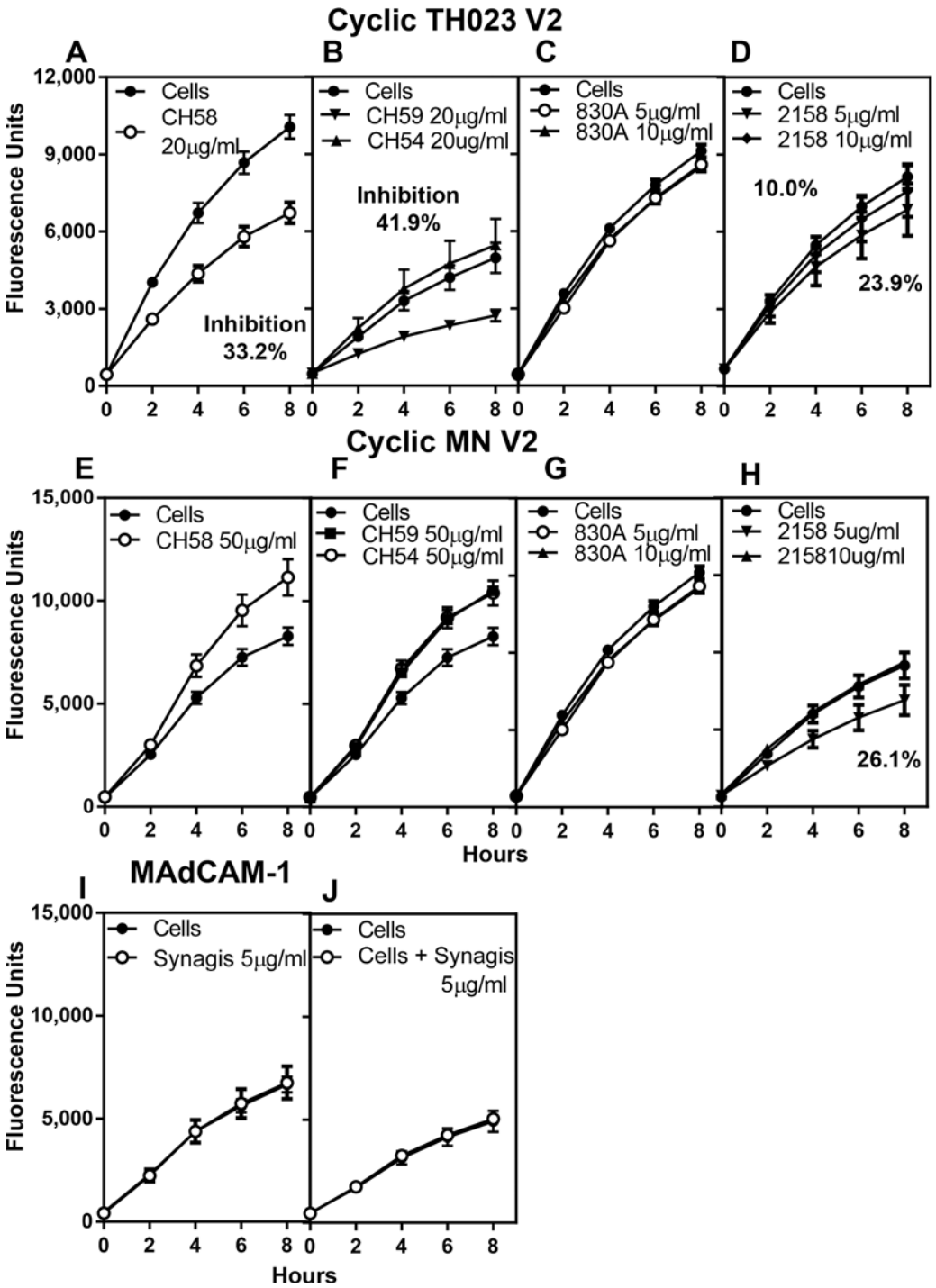

Fig 6. Inhibition of α4β7 integrin binding to cyclic V2 peptides by V2 mAbs. Human CH58, CH59, CH54, 830A, and 2158 mAbs were incubated with either cyclic V2 TH023 **(A-D)** or with cyclic V2 MN **(E-H)** peptides. CH58 **(A)**, CH59 **(B)** and 2158 **(D)** inhibit the binding of cyclic V2 TH023 peptide to α4β7 on RPMI8866 cells, while 830A **(C)** and a control mAb CH54 **(B)** did not inhibit the α4β7 binding. In contrast, only mAb 2158 **(H)** inhibited the binding of cyclic V2 MN to α4β7 on RPMI8866 cells. CH58 **(E)**, CH59 **(F)**, 830A **(H)** and CH54 **(F)** did not inhibit integrin binding to V2 MN. **(I and J)** Synagis®, a mAb specific to RSV was either incubated with the cells **(J)** and then added to MAdCAM-1 coated wells or **(I)** the mAb was added to MAdCAM-1 coated plates, followed by the addition of RPMI8866 cells. No inhibition of binding to α4β7 integrin was demonstrated in either case indicating the specificity of the assay. All experiments were performed 3 times. Each time point in graphs **A**, **B**, **E**, and **F**, represent the average fluorescence units ± S.D. of triplicate points of 3 experiments, while graphs **C**, **D**, **G**, **H**, **I**, and **J** are a representative plot of 3 experiments. The % inhibition if applicable is shown in the respective panels.

doi:10.1371/journal.pone.0143895.g006

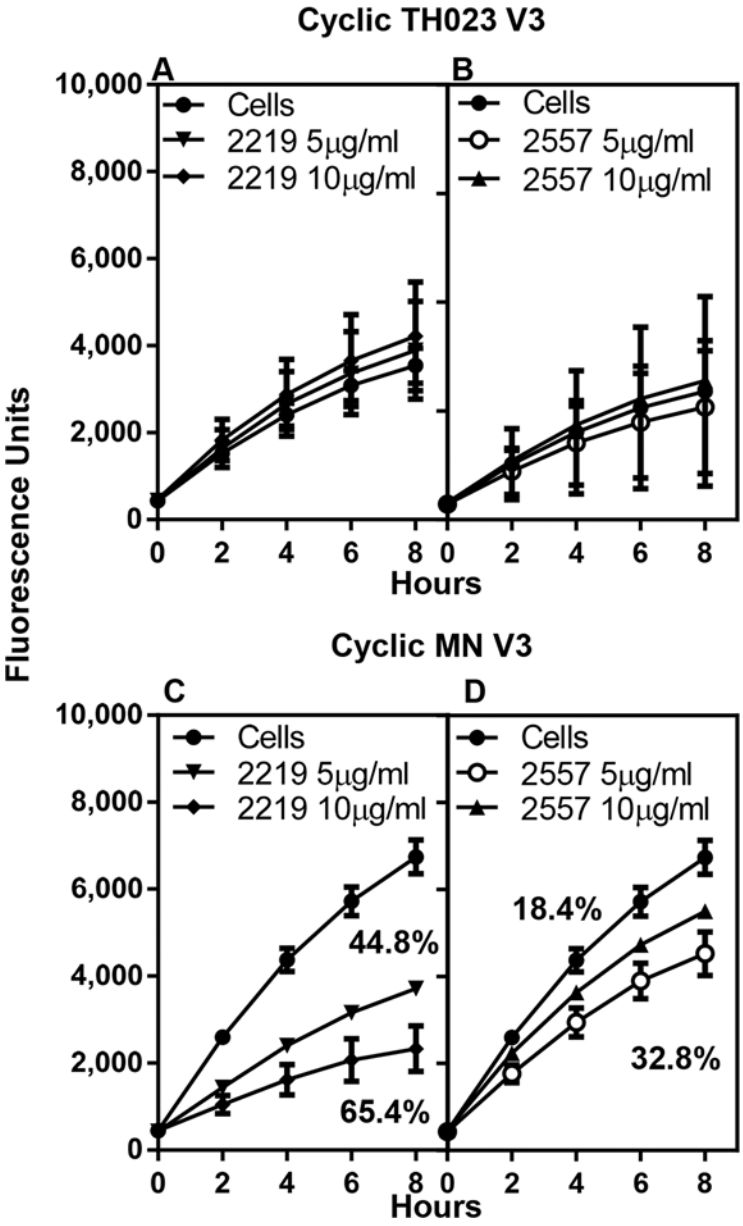

Fig 7. Inhibition of α4β7 integrin binding to cyclic V3 peptides by V3 mAbs. MAbs 2219 and 2557 were incubated with either cyclic V3 TH023 **(A and B)** or with cyclic V3 MN **(C and D)**. Neither mAbs 2219 **(A)** nor 2557 **(B)** inhibited the binding of cyclic V3 TH023 peptide to α4β7 on RPMI8866 cells. However, both mAb 2219 **(C)** and mAb 2557 **(D)** inhibited the binding of cyclic V3 MN to α4β7. Each time point represents the average fluorescence units of 2–3 experiments ± S.D. of triplicate points. The percent inhibition, if applicable, is shown in the respective panels.

doi:10.1371/journal.pone.0143895.g007

agreement with the results of Swetnam et al. [38] who showed that mAbs 2219 and 2557 bind CRF01_AE strains poorly, but recognize 70% of the circulating subtype B strains.

Inhibition of α4β7 binding to cyclic V2 peptides by plasma from naturally infected (CRF01_AE) individuals and by IgG from RV144 vaccinees

Plasma samples from Thai blood donors uninfected or infected with CRF01_AE virus were studied to determine if plasma from uninfected or naturally infected individuals could inhibit

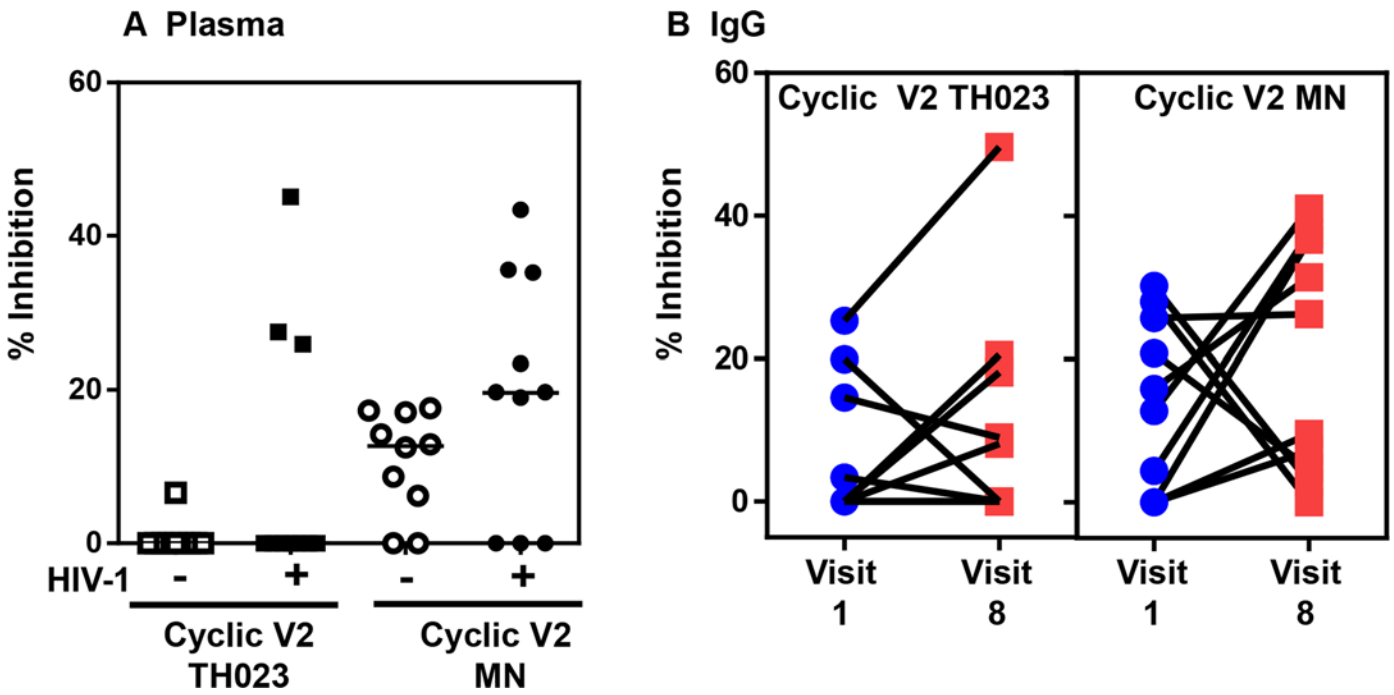

Fig 8. Plasma from uninfected, HIV-1-infected individuals, or purified IgG from uninfected RV144 vaccinees inhibit α4β7 integrin binding. Plasma (1:200 dilution) from Thai individuals uninfected or HIV-1 infected **(A)** or purified IgG from uninfected RV144 vaccinees **(B)** were incubated with cyclic V2 TH023 or MN peptides. **(A)** HIV-1 infected Thai individuals (3 out of 10) blocked the binding of α4β7 integrin to cyclic TH023 (closed squares). Plasma from uninfected (open circles) and infected individuals (closed circles) inhibited the binding of α4β7 integrin to cyclic MN V2 peptides to varying degrees; however the infected plasma exhibited higher levels of inhibition. **(B)** Purified IgG from uninfected RV144 vaccinees (post vaccination, Visit 8) inhibited the binding of α4β7 integrin to both TH023 and MN V2 peptides compared to pre-vaccination (Visit 1). The data shown are the mean of triplicate points.

doi:10.1371/journal.pone.0143895.g008

α4β7 on RMPI8866 cells from binding to either cyclic V2-TH023 or V2-MN peptides. Plasma samples from 10 volunteers (diluted 1:200) were individually incubated with either cyclic V2-TH023 or V2-MN peptide-coated plates, washed, and followed by the addition of RPMI8866 cells (Fig 8A). The inhibition ranged from 0–45%. As expected, a higher degree of inhibition was obtained with plasma from infected compared to uninfected individuals.

Next we studied the ability of purified IgG from 10 uninfected RV144 vaccinees, pre (visit 1) and week 26 (2 weeks after last vaccination, visit 8), to inhibit α4β7 integrin binding to cyclic V2 TH023 and MN peptides (Fig 8B). Two different concentrations of purified IgG, 10 μg/ml and 20 μg/ml, were tested and the data from the 10 μg/ml is shown. Purified IgG inhibited cyclic TH023 and MN V2 peptide binding to α4β7 integrin receptor to varying levels in 4 and 6 out of the 10 vaccinees, respectively. Inhibition with purified IgG was also observed with V3 TH023 but not with V3 MN peptides (data not shown).

Discussion

The α4β7 integrin receptor on the surface of T cells has been shown to interact with the V2 loop through the LDI/V motif [8]. CryoEM data suggest that the HIV-1 gp120 V1/V2 domain is located at the tip of the envelope spike, ~150 Å from the virus envelope thus favorably positioning it for receptor interactions. The α4β7 integrin receptor is about 3-times further extended than the primary CD4 receptor and hence readily accessible to capture the virus [39].

The RV144 immune correlates study has directed the focus of the HIV-1 field to the V1V2 and V3 regions of HIV-1 envelope protein gp120 [3–5]. However, the mechanism by which these antibodies exert their protection is currently unknown. It has been postulated that

antibodies that bind to or near the integrin α4β7-binding motif probably interfere with the gp120-α4β7 interaction and prevent viral transmission [23, 40]. However, studies showing a lack of detectable α4β7 binding to HIV-1 virions and gp120 envelope proteins argue against this homing receptor being critical for mucosal HIV-1 transmission [41, 42]. In contrast, studies by Nakamura et al [43] demonstrated that antibodies to the V2 domain inhibited the binding of rgp120 to α4β7. Recently another region within the V2 loop (aa 170–172) has been identified that affects integrin binding to gp120 [44]. *In vivo* studies in rhesus macaques have demonstrated that targeting α4β7 by administering an anti-α4β7 monoclonal antibody during acute infection reduces mucosal transmission of SIV $_{mac251}$ [20, 22].

Both in vitro and SIV transmission /infection studies have their own limitations. In the host mucosa, the virus has to be captured from a relatively small inoculum in a short period of time and the initial interactions between the viral envelope, CD4, and α4β7 might be crucial. The current *in vitro* assay that utilizes primary $CD4^+$ T cells [45] for the detection of antibodies that bind to α4β7 must induce the active form of α4β7 with retinoic acid and block the CD4 receptor with anti-CD4 antibody in order to distinguish α4β7 binding from CD4 binding [8]. Theoretically, the number of α4β7 and CD4 receptors could vary depending upon the donor and the concentration of retinoic acid used. Studies utilizing a viral replication inhibition assay have suggested a role for α4β7 in HIV infection, which is influenced not only by the sequence of the α4β7 binding motif but also by other viral and host factors [46]. Several studies have used anti-α4 or anti-β7 antibody [41, 42, 47] to demonstrate the lack of interaction between α4β7 integrin receptor and gp120 or virions. However, these antibodies may not bind the activated form of α4β7 integrin receptor. To our knowledge, ACT-1 is the only mAb that is capable of binding all forms of the activated α4β7 integrin receptor.

In the RV144 Phase III trial, the majority of the antibody responses to the V2 region were directed against the mid-region of the V2 loop, which included the LDI/V motif [1]. Antibody responses to the cyclic V2 SFL peptide as measured by ELISA or Biacore were almost identical to those against the wild type cyclic V2 peptide, indicating that the majority of V2 antibody responses were localized within this region. Scrambling the amino acid sequences of the mid-region of the V2 loop (SMR) significantly reduced the magnitude and frequency of antibody binding with only 50% of the plasma samples being above background values [6]. However unlike the RV144 ELISA/Biacore binding data mentioned above, both the SFL and SMR V2 peptides specifically inhibited (35–40%) the binding of α4β7 to MAdCAM-1 as shown by the absence of inhibition by the completely scrambled V2 peptide (SCR). Thus, these data suggest that in addition to the mid region, amino acid sequences in the flanking region can also influence the V2-α4β7 interaction.

Surprisingly, both MN and TH023 V3 peptides strongly inhibited (80%) the binding of MAdCAM-1 to α4β7 receptors. The inhibition was specific as the interaction could be blocked by ACT-1. The MN and TH023 V3 peptide sequences vary considerably between each other and their respective V2 sequences, thus providing additional support that besides the LDI motif, other regions in V2 and V3 are important for the α4β7-V2/V3 interaction. The binding could be due to charged amino acids and/or discontinuous epitopes in the highly dynamic V2/V3 loop regions. The direct intramolecular interaction between V2 and V3 loops stabilized by sulfated tyrosines within the V2 loop is further supported by biological and structural studies [48, 49]. Furthermore, the conformational flexibility of the V2 region is demonstrated by the different structures adopted when it is complexed with mAbs. V2 exists as an α-helical structure or as a coil when it is bound by CH58 or CH59, while it is in a β strand structure when bound by the mAb PG9 [33, 50]. Not only does the V2 exhibit multiple conformations, but the α4β7 receptor also exhibits at least 3 different conformations, which are in a dynamic flux [51] further contributing to the complexity of the α4β7 receptor-gp120 interaction.

Inhibition of $\alpha_4\beta_7$ binding has been demonstrated with a panel of V2-specific mouse mAbs whose epitopes overlap the integrin-binding site [43]. The RV144-derived V2-specific mAbs, CH58 and CH59 recognize a continuous linear region of V2, amino acids 167–181 and 168–173 respectively, are glycan independent, and bind both monomeric gp120 and V2 peptides [33]. In our study, both CH58 and CH59 inhibited the binding of TH023 but not MN V2 peptides to α4β7 receptors.

Recently Mayr et al [52] and Upadhya et al. [36], have described the epitope and function of a set of mAbs designated as variable loop V2 integrin (V2i)-specific antibodies. V2i epitopes require proper conformation of the V1V2 domain and map to the disordered V2 loop that connects the C and D strands, in particular, the area overlapping with the integrin α4β7-binding site [53]. We tested two of these V2i mAbs, 830A and 2158 [52, 53] to determine if they could inhibit α4β7-binding. Although, these V2i mAbs do not bind to linear V2 peptides, similar to others previously described [37], in our study a modest inhibition was observed with mAb 2158. This is probably due to mAb 2158 binding poorly to the cyclic V2 peptide.

Anti-V3 antibodies are present in the sera of virtually all individuals infected with HIV-1 [54, 55]. Several V3-specific human mAbs have been produced [56–58] and these mainly target the crown region of V3 [59, 60]. Two of the V3 human mAbs, 2219 and 2257 that recognize epitopes in the crown region, aa 304–318 (see Table 1), specifically inhibited (65% and 33%, respectively) the V3 MN binding but not the V3 TH023 binding to the α4β7 integrin receptor. The lysine (K) residue at position 305 in the V3 peptide appears to be important to form potential salt bridges with the mAbs. Lysine is replaced by tyrosine (T) in V3 TH023 peptide and this amino acid change could be the reason for the observed lack of inhibition of the V3 TH023 peptide binding to the α4β7 integrin receptor by the two mAbs tested in our study. This would also suggest that residues 304–318 of the V3 loop are involved in binding to the α4β7 integrin receptor.

Based on neutralization data, it is believed that V1V2 and V3 epitopes are not readily accessible on the envelope spikes [36, 61]. Recently published trimeric HIV-1 envelope structures [62–65] and previously published electron tomography and cryoelectron microscopy studies [63, 66–68] have revealed that V1V2 is located at the apex of the unliganded trimer and should theoretically be accessible to anti-V2 antibodies, while the V3 loop is tucked below the V1V2 with the crown region facing away from the trimer surface. However, it is important to know if the V2 and V3 regions are accessible on the surface of the virions to interact with α4β7 integrin receptor. Therefore, we assessed the ability of primary HIV-1 and full-length IMCs from acute and chronic HIV-1 to inhibit the binding of α4β7 receptors to MAdCAM-1. Tier 1 viruses in general have a more open conformation of the trimers, with the V2 and V3 regions being more accessible to binding ligands. BaL, a subtype B virus has been shown to bind to both activated $CD4^+$ T cells as well as cell lines stably expressing α4β7. The binding as well as the infectivity of α4β7-activated $CD4^+$ T cells was decreased in the presence of anti- α4β7 antibodies [69]. Of the 4 subtype B tier 1 primary viruses tested in our assay, two of the viruses, SF162 and TH023 inhibited the binding in a dose-dependent manner, while US-1 and JRFL did not. JRFL gp120 and JRFL pseudovirus have been previously shown not to bind α4β7 or inhibit infection in the presence of mAbs ACT-1 or α4 specific mAb 2B4 [40, 41], while SF162 has been shown to inhibit the binding and infection [41] of the trimers, with the V2 and V3 regions being more accessible to binding ligands.

The two primary subtype B viruses, SF162 and TH023, that were able to inhibit α4β7-binding in our study are predicted to have a coiled structure and an α-helix in the 166–169 region of V2 while JRFL and US-1 that did not inhibit do not have a predicted coiled structure or α-helix. JRFL and US-1 are predicted to have a broken α-helix structure and a β-turn structure, respectively. This specific amino acid region of V2 contains both the sieve mutation at position

169 [35] and a cryptic determinant of α4β7 integrin binding (aa166-178). Coincidentally, all of the IMC's tested in our system are predicted to have α-helixes at residures166-169. Furthermore, in our assay, acute and chronic CRF01_AE, and C showed a trend of higher inhibition with increasing concentrations of the virus. In all likelihood, the predicted structures alone are not then the only measure of α4β7 integrin inhibition, but rather a range of factors including amino acid charge that could also contribute to the binding/inhibition.

During the course of HIV-1 infection, binding antibodies to various regions of the envelope protein are induced. Our studies indicate that plasma from chronic HIV-1 infected individuals contain antibodies directed against the V2 region that inhibit the binding of α4β7 to the V2 peptides to varying degrees. Interestingly, purified IgG from RV144 vaccinees also inhibited the binding of α4β7 to V2 TH023 and MN peptides, demonstrating that vaccination can induce these types of antibodies.

Conclusion

Besides the known LDI motif, our study demonstrates previously unidentified regions in HIV-1 V2 and V3 loops that are important in α4β7 binding. As has been previously suggested, a combination of structure and charge within V2 may be the critical features modulating the effect of the α4β7-gp120 interaction. V2- and V3-specific binding mAbs were able to block the α4β7 binding. Epitopes involved in binding to the α4β7 region were accessible on PBMC produced primary infectious viruses and on acute infectious molecular clone viruses. From these data, we hypothesize that early induction of V2 specific antibodies targeting the α4β7 region as a result of vaccination can play a role in viral acquisition. Understanding the interaction of V2 and V3 regions of HIV-1 envelope with α4β7 will contribute to the selection and design of immunogens that can induce antibodies to these regions with protective functions.

Supporting Information

S1 Data. Flow Cytometry Raw Data for Fig 1A APC-α4β7.
(FCS)

S2 Data. Flow Cytometry Raw Data for Fig 1A Isotype Control.
(FCS)

S3 Data. Flow Cytometry Raw Data for Fig 1A Unstained.
(FCS)

S4 Data. Flow Cytometry Raw Data for Fig 1B Goat-anti-mouse IgG Texas Red.
(FCS)

S5 Data. Flow Cytometry Raw Data for Fig 1B gp120 Protein.
(FCS)

S6 Data. Flow Cytometry Raw Data for Fig 1C Scrambled V2 Peptide 1μg.
(FCS)

S7 Data. Flow Cytometry Raw Data for Fig 1C 92TH023 V2 Peptide 1μg.
(FCS)

S8 Data. Flow Cytometry Raw Data for Fig 1C Unstained Cells.
(FCS)

S9 Data. Flow Cytometry Raw Data for Fig 1C Scrambled V2 Peptide 5μg.
(FCS)

S10 Data. Flow Cytometry Raw Data for Fig 1C 92TH023 V2 Peptide 5μg.
(FCS)

Acknowledgments

The authors thank Jiae Kim for reading the manuscript and providing comments and Michael Eller for flow core facilities. Human monoclonal antibodies CH54, CH58, and CH59 isolated from RV144 vaccinees were kindly provided by Dr. Barton Haynes, Duke Human Vaccine Institute, Duke University Medical Center, Durham, NC, USA.

Disclaimer: The views expressed in this article are those of the authors and do not reflect the official policy of the Department of the Army, Department of Defense, or the U.S. Government.

Author Contributions

Conceived and designed the experiments: MR KKP CRA. Performed the experiments: KKP. Analyzed the data: KKP MR. Contributed reagents/materials/analysis tools: A-LC RM ST SZ-P NK SR-N KJ SN PP NLM JHK. Wrote the paper: KKP MR.

References

1. Haynes BF, Gilbert PB, McElrath MJ, Zolla-Pazner S, Tomaras GD, Alam SM, et al. Immune-correlates analysis of an HIV-1 vaccine efficacy trial. N Engl J Med. 2012; 366(14):1275–86. doi: 10.1056/NEJMoa1113425 PMID: 22475592; PubMed Central PMCID: PMC3371689.
2. Gottardo R, Bailer RT, Korber BT, Gnanakaran S, Phillips J, Shen X, et al. Plasma IgG to linear epitopes in the V2 and V3 regions of HIV-1 gp120 correlate with a reduced risk of infection in the RV144 vaccine efficacy trial. PLoS One. 2013; 8(9):e75665. doi: 10.1371/journal.pone.0075665 PMID: 24086607; PubMed Central PMCID: PMC3784573.
3. Zolla-Pazner S, deCamp A, Gilbert PB, Williams C, Yates NL, Williams WT, et al. Vaccine-induced IgG antibodies to V1V2 regions of multiple HIV-1 subtypes correlate with decreased risk of HIV-1 infection. PLoS One. 2014; 9(2):e87572. doi: 10.1371/journal.pone.0087572 PMID: 24504509; PubMed Central PMCID: PMC3913641.
4. Zolla-Pazner S, deCamp AC, Cardozo T, Karasavvas N, Gottardo R, Williams C, et al. Analysis of V2 antibody responses induced in vaccinees in the ALVAC/AIDSVAX HIV-1 vaccine efficacy trial. PLoS One. 2013; 8(1):e53629. doi: 10.1371/journal.pone.0053629 PMID: 23349725; PubMed Central PMCID: PMC3547933.
5. Zolla-Pazner S, Edlefsen PT, Rolland M, Kong XP, deCamp A, Gottardo R, et al. Vaccine-induced Human Antibodies Specific for the Third Variable Region of HIV-1 gp120 Impose Immune Pressure on Infecting Viruses. EBioMedicine. 2014; 1(1):37–45. doi: 10.1016/j.ebiom.2014.10.022 PMID: 25599085; PubMed Central PMCID: PMC4293639.
6. Karasavvas N, Billings E, Rao M, Williams C, Zolla-Pazner S, Bailer RT, et al. The Thai Phase III HIV Type 1 Vaccine trial (RV144) regimen induces antibodies that target conserved regions within the V2 loop of gp120. AIDS Res Hum Retroviruses. 2012; 28(11):1444–57. doi: 10.1089/aid.2012.0103 PMID: 23035746; PubMed Central PMCID: PMC3484815.
7. Yates NL, Liao HX, Fong Y, deCamp A, Vandergrift NA, Williams WT, et al. Vaccine-induced Env V1-V2 IgG3 correlates with lower HIV-1 infection risk and declines soon after vaccination. Sci Transl Med. 2014; 6(228):228ra39. doi: 10.1126/scitranslmed.3007730 PMID: 24648342; PubMed Central PMCID: PMC4116665.
8. Arthos J, Cicala C, Martinelli E, Macleod K, Van Ryk D, Wei D, et al. HIV-1 envelope protein binds to and signals through integrin alpha4beta7, the gut mucosal homing receptor for peripheral T cells. Nat Immunol. 2008; 9(3):301–9. doi: 10.1038/ni1566 PMID: 18264102.
9. Cicala C, Martinelli E, McNally JP, Goode DJ, Gopaul R, Hiatt J, et al. The integrin alpha4beta7 forms a complex with cell-surface CD4 and defines a T-cell subset that is highly susceptible to infection by HIV-1. Proc Natl Acad Sci U S A. 2009; 106(49):20877–82. doi: 10.1073/pnas.0911796106 PMID: 19933330; PubMed Central PMCID: PMC2780317.
10. Hynes RO. Integrins: bidirectional, allosteric signaling machines. Cell. 2002; 110(6):673–87. PMID: 12297042.

11. Butcher EC, Picker LJ. Lymphocyte homing and homeostasis. Science. 1996; 272(5258):60–6. PMID: 8600538.
12. Luo BH, Springer TA. Integrin structures and conformational signaling. Curr Opin Cell Biol. 2006; 18 (5):579–86. doi: 10.1016/j.ceb.2006.08.005 PMID: 16904883; PubMed Central PMCID: PMC1618925.
13. Yu Y, Zhu J, Mi LZ, Walz T, Sun H, Chen J, et al. Structural specializations of alpha(4)beta(7), an integrin that mediates rolling adhesion. J Cell Biol. 2012; 196(1):131–46. doi: 10.1083/jcb.201110023 PMID: 22232704; PubMed Central PMCID: PMC3255974.
14. Jolly C, Kashefi K, Hollinshead M, Sattentau QJ. HIV-1 cell to cell transfer across an Env-induced, actin-dependent synapse. J Exp Med. 2004; 199(2):283–93. doi: 10.1084/jem.20030648 PMID: 14734528; PubMed Central PMCID: PMC2211771.
15. Bromley SK, Burack WR, Johnson KG, Somersalo K, Sims TN, Sumen C, et al. The immunological synapse. Annu Rev Immunol. 2001; 19:375–96. doi: 10.1146/annurev.immunol.19.1.375 PMID: 11244041.
16. Haase AT. Perils at mucosal front lines for HIV and SIV and their hosts. Nat Rev Immunol. 2005; 5 (10):783–92. doi: 10.1038/nri1705 PMID: 16200081.
17. Rao M, Peachman KK, Kim J, Gao G, Alving CR, Michael NL, et al. HIV-1 variable loop 2 and its importance in HIV-1 infection and vaccine development. Curr HIV Res. 2013; 11(5):427–38. PMID: 24191938; PubMed Central PMCID: PMC4086350.
18. Danner R, Chaudhari SN, Rosenberger J, Surls J, Richie TL, Brumeanu TD, et al. Expression of HLA class II molecules in humanized NOD.Rag1KO.IL2RgcKO mice is critical for development and function of human T and B cells. PLoS One. 2011; 6(5):e19826. doi: 10.1371/journal.pone.0019826 PMID: 21611197; PubMed Central PMCID: PMC3096643.
19. Allam A, Majji S, Peachman K, Jagodzinski L, Kim J, Ratto-Kim S, et al. TFH cells accumulate in mucosal tissues of humanized-DRAG mice and are highly permissive to HIV-1. Sci Rep. 2015; 5:10443. doi: 10.1038/srep10443 PMID: 26034905.
20. Ansari AA, Reimann KA, Mayne AE, Takahashi Y, Stephenson ST, Wang R, et al. Blocking of alpha4-beta7 gut-homing integrin during acute infection leads to decreased plasma and gastrointestinal tissue viral loads in simian immunodeficiency virus-infected rhesus macaques. J Immunol. 2011; 186 (2):1044–59. doi: 10.4049/jimmunol.1003052 PMID: 21149598; PubMed Central PMCID: PMC3691699.
21. Martinelli E, Veglia F, Goode D, Guerra-Perez N, Aravantinou M, Arthos J, et al. The frequency of alpha (4)beta(7)(high) memory CD4(+) T cells correlates with susceptibility to rectal simian immunodeficiency virus infection. J Acquir Immune Defic Syndr. 2013; 64(4):325–31. doi: 10.1097/QAI.0b013e31829f6e1a PMID: 23797688; PubMed Central PMCID: PMC3815485.
22. Byrareddy SN, Kallam B, Arthos J, Cicala C, Nawaz F, Hiatt J, et al. Targeting alpha4beta7 integrin reduces mucosal transmission of simian immunodeficiency virus and protects gut-associated lymphoid tissue from infection. Nat Med. 2014; 20(12):1397–400. doi: 10.1038/nm.3715 PMID: 25419708; PubMed Central PMCID: PMC4257865.
23. Cicala C, Arthos J, Fauci AS. HIV-1 envelope, integrins and co-receptor use in mucosal transmission of HIV. Journal of Translational Medicine. 2010; 9(Suppl 1).
24. Montefiori DC, Karnasuta C, Huang Y, Ahmed H, Gilbert P, de Souza MS, et al. Magnitude and breadth of the neutralizing antibody response in the RV144 and Vax003 HIV-1 vaccine efficacy trials. J Infect Dis. 2012; 206(3):431–41. doi: 10.1093/infdis/jis367 PMID: 22634875; PubMed Central PMCID: PMC3392187.
25. Barouch DH, Liu J, Li H, Maxfield LF, Abbink P, Lynch DM, et al. Vaccine protection against acquisition of neutralization-resistant SIV challenges in rhesus monkeys. Nature. 2012; 482(7383):89–93. doi: 10.1038/nature10766 PMID: 22217938; PubMed Central PMCID: PMC3271177.
26. Pegu P, Vaccari M, Gordon S, Keele BF, Doster M, Guan Y, et al. Antibodies with high avidity to the gp120 envelope protein in protection from simian immunodeficiency virus SIV(mac251) acquisition in an immunization regimen that mimics the RV-144 Thai trial. J Virol. 2013; 87(3):1708–19. doi: 10.1128/JVI.02544-12 PMID: 23175374; PubMed Central PMCID: PMC3554145.
27. Rerks-Ngarm S, Pitisuttithum P, Nitayaphan S, Kaewkungwal J, Chiu J, Paris R, et al. Vaccination with ALVAC and AIDSVAX to prevent HIV-1 infection in Thailand. N Engl J Med. 2009; 361(23):2209–20. doi: 10.1056/NEJMoa0908492 PMID: 19843557.
28. Wei X, Decker JM, Liu H, Zhang Z, Arani RB, Kilby JM, et al. Emergence of resistant human immunodeficiency virus type 1 in patients receiving fusion inhibitor (T-20) monotherapy. Antimicrob Agents Chemother. 2002; 46(6):1896–905. PMID: 12019106; PubMed Central PMCID: PMC127242.
29. Wei X, Decker JM, Wang S, Hui H, Kappes JC, Wu X, et al. Antibody neutralization and escape by HIV-1. Nature. 2003; 422(6929):307–12. doi: 10.1038/nature01470 PMID: 12646921.

30. McLinden RJ, Labranche CC, Chenine AL, Polonis VR, Eller MA, Wieczorek L, et al. Detection of HIV-1 neutralizing antibodies in a human CD4(+)/CXCR4(+)/CCR5(+) T-lymphoblastoid cell assay system. PLoS One. 2013; 8(11):e77756. doi: 10.1371/journal.pone.0077756 PMID: 24312168; PubMed Central PMCID: PMC3842913.

31. Chenine AL, Wieczorek L, Sanders-Buell E, Wesberry M, Towle T, Pillis DM, et al. Impact of HIV-1 backbone on neutralization sensitivity: neutralization profiles of heterologous envelope glycoproteins expressed in native subtype C and CRF01_AE backbone. PLoS One. 2013; 8(11):e76104. Epub 2013/12/07. doi: 10.1371/journal.pone.0076104 PONE-D-13-17876 [pii]. PMID: 24312165; PubMed Central PMCID: PMC3843658.

32. Jobe O, Peachman KK, Matyas GR, Asher LV, Alving CR, Rao M. An anti-phosphoinositide-specific monoclonal antibody that neutralizes HIV-1 infection of human monocyte-derived macrophages. Virology. 2012; 430(2):110–9. doi: 10.1016/j.virol.2012.04.017 PMID: 22633000.

33. Liao HX, Bonsignori M, Alam SM, McLellan JS, Tomaras GD, Moody MA, et al. Vaccine induction of antibodies against a structurally heterogeneous site of immune pressure within HIV-1 envelope protein variable regions 1 and 2. Immunity. 2013; 38(1):176–86. doi: 10.1016/j.immuni.2012.11.011 PMID: 23313589; PubMed Central PMCID: PMC3569735.

34. Soler D, Chapman T, Yang LL, Wyant T, Egan R, Fedyk ER. The binding specificity and selective antagonism of vedolizumab, an anti-alpha4beta7 integrin therapeutic antibody in development for inflammatory bowel diseases. J Pharmacol Exp Ther. 2009; 330(3):864–75. doi: 10.1124/jpet.109.153973 PMID: 19509315.

35. Rolland M, Edlefsen PT, Larsen BB, Tovanabutra S, Sanders-Buell E, Hertz T, et al. Increased HIV-1 vaccine efficacy against viruses with genetic signatures in Env V2. Nature. 2012; 490(7420):417–20. doi: 10.1038/nature11519 PMID: 22960785; PubMed Central PMCID: PMC3551291.

36. Upadhyay C, Mayr LM, Zhang J, Kumar R, Gorny MK, Nadas A, et al. Distinct mechanisms regulate exposure of neutralizing epitopes in the V2 and V3 loops of HIV-1 envelope. J Virol. 2014; 88(21):12853–65. doi: 10.1128/JVI.02125-14 PMID: 25165106; PubMed Central PMCID: PMC4248937.

37. Gorny MK, Moore JP, Conley AJ, Karwowska S, Sodroski J, Williams C, et al. Human anti-V2 monoclonal antibody that neutralizes primary but not laboratory isolates of human immunodeficiency virus type 1. J Virol. 1994; 68(12):8312–20. PMID: 7525987; PubMed Central PMCID: PMC237300.

38. Swetnam J, Shmelkov E, Zolla-Pazner S, Cardozo T. Comparative magnitude of cross-strain conservation of HIV variable loop neutralization epitopes. PLoS One. 2010; 5(12):e15994. doi: 10.1371/journal.pone.0015994 PMID: 21209919; PubMed Central PMCID: PMC3012121.

39. Cicala C, Arthos J, Fauci AS. HIV-1 envelope, integrins and co-receptor use in mucosal transmission of HIV. J Transl Med. 2011; 9 Suppl 1:S2. doi: 10.1186/1479-5876-9-S1-S2 PMID: 21284901; PubMed Central PMCID: PMC3105502.

40. Nawaz F, Cicala C, Van Ryk D, Block KE, Jelicic K, McNally JP, et al. The genotype of early-transmitting HIV gp120s promotes alpha (4) beta(7)-reactivity, revealing alpha (4) beta(7) +/CD4+ T cells as key targets in mucosal transmission. PLoS Pathog. 2011; 7(2):e1001301. doi: 10.1371/journal.ppat.1001301 PMID: 21383973; PubMed Central PMCID: PMC3044691.

41. Parrish NF, Wilen CB, Banks LB, Iyer SS, Pfaff JM, Salazar-Gonzalez JF, et al. Transmitted/founder and chronic subtype C HIV-1 use CD4 and CCR5 receptors with equal efficiency and are not inhibited by blocking the integrin alpha4beta7. PLoS Pathog. 2012; 8(5):e1002686. doi: 10.1371/journal.ppat.1002686 PMID: 22693444; PubMed Central PMCID: PMC3364951.

42. Perez LG, Chen H, Liao HX, Montefiori DC. Envelope glycoprotein binding to the integrin alpha4beta7 is not a general property of most HIV-1 strains. J Virol. 2014; 88(18):10767–77. doi: 10.1128/JVI.03296-13 PMID: 25008916; PubMed Central PMCID: PMC4178844.

43. Nakamura GR, Fonseca DP, O'Rourke SM, Vollrath AL, Berman PW. Monoclonal antibodies to the V2 domain of MN-rgp120: fine mapping of epitopes and inhibition of alpha4beta7 binding. PLoS One. 2012; 7(6):e39045. doi: 10.1371/journal.pone.0039045 PMID: 22720026; PubMed Central PMCID: PMC3374778.

44. Tassaneetrithep B, Tivon D, Swetnam J, Karasavvas N, Michael NL, Kim JH, et al. Cryptic determinant of alpha4beta7 binding in the V2 loop of HIV-1 gp120. PLoS One. 2014; 9(9):e108446. doi: 10.1371/journal.pone.0108446 PMID: 25265384; PubMed Central PMCID: PMC4180765.

45. Arthos J, Deen KC, Chaikin MA, Fornwald JA, Sathe G, Sattentau QJ, et al. Identification of the residues in human CD4 critical for the binding of HIV. Cell. 1989; 57(3):469–81. PMID: 2541915.

46. Richardson SI, Gray ES, Mkhize NN, Sheward DJ, Lambson BE, Wibmer CK, et al. South African HIV-1 subtype C transmitted variants with a specific V2 motif show higher dependence on alpha4beta7 for replication. Retrovirology. 2015; 12:54. doi: 10.1186/s12977-015-0183-3 PMID: 26105197; PubMed Central PMCID: PMC4479312.

47. Pauls E, Ballana E, Moncunill G, Bofill M, Clotet B, Ramo-Tello C, et al. Evaluation of the anti-HIV activity of natalizumab, an antibody against integrin alpha4. AIDS. 2009; 23(2):266–8. PMID: 19112691.

48. Cimbro R, Gallant TR, Dolan MA, Guzzo C, Zhang P, Lin Y, et al. Tyrosine sulfation in the second variable loop (V2) of HIV-1 gp120 stabilizes V2-V3 interaction and modulates neutralization sensitivity. Proc Natl Acad Sci U S A. 2014; 111(8):3152–7. doi: 10.1073/pnas.1314718111 PMID: 24569807; PubMed Central PMCID: PMC3939864.

49. Totrov M. Estimated secondary structure propensities within V1/V2 region of HIV gp120 are an important global antibody neutralization sensitivity determinant. PLoS One. 2014; 9(4):e94002. doi: 10.1371/journal.pone.0094002 PMID: 24705879; PubMed Central PMCID: PMC3976368.

50. McLellan JS, Pancera M, Carrico C, Gorman J, Julien JP, Khayat R, et al. Structure of HIV-1 gp120 V1/V2 domain with broadly neutralizing antibody PG9. Nature. 2011; 480(7377):336–43. doi: 10.1038/nature10696 PMID: 22113616; PubMed Central PMCID: PMC3406929.

51. Yu Y, Schurpf T, Springer TA. How natalizumab binds and antagonizes alpha4 integrins. J Biol Chem. 2013; 288(45):32314–25. doi: 10.1074/jbc.M113.501668 PMID: 24047894; PubMed Central PMCID: PMC3820868.

52. Mayr LM, Cohen S, Spurrier B, Kong XP, Zolla-Pazner S. Epitope mapping of conformational V2-specific anti-HIV human monoclonal antibodies reveals an immunodominant site in V2. PLoS One. 2013; 8(7):e70859. doi: 10.1371/journal.pone.0070859 PMID: 23923028; PubMed Central PMCID: PMC3726596.

53. Spurrier B, Sampson J, Gorny MK, Zolla-Pazner S, Kong XP. Functional implications of the binding mode of a human conformation-dependent V2 monoclonal antibody against HIV. J Virol. 2014; 88(8):4100–12. doi: 10.1128/JVI.03153-13 PMID: 24478429; PubMed Central PMCID: PMC3993739.

54. Carrow EW, Vujcic LK, Glass WL, Seamon KB, Rastogi SC, Hendry RM, et al. High prevalence of antibodies to the gp120 V3 region principal neutralizing determinant of HIV-1MN in sera from Africa and the Americas. AIDS Res Hum Retroviruses. 1991; 7(10):831–8. PMID: 1720630.

55. Krachmarov CP, Kayman SC, Honnen WJ, Trochev O, Pinter A. V3-specific polyclonal antibodies affinity purified from sera of infected humans effectively neutralize primary isolates of human immunodeficiency virus type 1. AIDS Res Hum Retroviruses. 2001; 17(18):1737–48. doi: 10.1089/08892220152741432 PMID: 11788025.

56. Scheid JF, Mouquet H, Feldhahn N, Seaman MS, Velinzon K, Pietzsch J, et al. Broad diversity of neutralizing antibodies isolated from memory B cells in HIV-infected individuals. Nature. 2009; 458(7238):636–40. doi: 10.1038/nature07930 PMID: 19287373.

57. Corti D, Langedijk JP, Hinz A, Seaman MS, Vanzetta F, Fernandez-Rodriguez BM, et al. Analysis of memory B cell responses and isolation of novel monoclonal antibodies with neutralizing breadth from HIV-1-infected individuals. PLoS One. 2010; 5(1):e8805. doi: 10.1371/journal.pone.0008805 PMID: 20098712; PubMed Central PMCID: PMC2808385.

58. Jiang X, Burke V, Totrov M, Williams C, Cardozo T, Gorny MK, et al. Conserved structural elements in the V3 crown of HIV-1 gp120. Nat Struct Mol Biol. 2010; 17(8):955–61. doi: 10.1038/nsmb.1861 PMID: 20622876.

59. Zolla-Pazner S, Zhong P, Revesz K, Volsky B, Williams C, Nyambi P, et al. The cross-clade neutralizing activity of a human monoclonal antibody is determined by the GPGR V3 motif of HIV type 1. AIDS Res Hum Retroviruses. 2004; 20(11):1254–8. doi: 10.1089/0889222042545054 PMID: 15588347.

60. Stanfield RL, Gorny MK, Zolla-Pazner S, Wilson IA. Crystal structures of human immunodeficiency virus type 1 (HIV-1) neutralizing antibody 2219 in complex with three different V3 peptides reveal a new binding mode for HIV-1 cross-reactivity. J Virol. 2006; 80(12):6093–105. doi: 10.1128/JVI.00205-06 PMID: 16731948; PubMed Central PMCID: PMC1472588.

61. Shotton C, Arnold C, Sattentau Q, Sodroski J, McKeating JA. Identification and characterization of monoclonal antibodies specific for polymorphic antigenic determinants within the V2 region of the human immunodeficiency virus type 1 envelope glycoprotein. J Virol. 1995; 69(1):222–30. PMID: 7527084; PubMed Central PMCID: PMC188567.

62. Lyumkis D, Julien JP, de Val N, Cupo A, Potter CS, Klasse PJ, et al. Cryo-EM structure of a fully glycosylated soluble cleaved HIV-1 envelope trimer. Science. 2013; 342(6165):1484–90. doi: 10.1126/science.1245627 PMID: 24179160; PubMed Central PMCID: PMC3954647.

63. Julien JP, Cupo A, Sok D, Stanfield RL, Lyumkis D, Deller MC, et al. Crystal structure of a soluble cleaved HIV-1 envelope trimer. Science. 2013; 342(6165):1477–83. doi: 10.1126/science.1245625 PMID: 24179159; PubMed Central PMCID: PMC3886632.

64. Bartesaghi A, Merk A, Borgnia MJ, Milne JL, Subramaniam S. Prefusion structure of trimeric HIV-1 envelope glycoprotein determined by cryo-electron microscopy. Nat Struct Mol Biol. 2013; 20(12):1352–7. doi: 10.1038/nsmb.2711 PMID: 24154805; PubMed Central PMCID: PMC3917492.

65. Khayat R, Lee JH, Julien JP, Cupo A, Klasse PJ, Sanders RW, et al. Structural characterization of cleaved, soluble HIV-1 envelope glycoprotein trimers. J Virol. 2013; 87(17):9865–72. doi: 10.1128/JVI.01222-13 PMID: 23824817; PubMed Central PMCID: PMC3754114.

66. Liu J, Bartesaghi A, Borgnia MJ, Sapiro G, Subramaniam S. Molecular architecture of native HIV-1 gp120 trimers. Nature. 2008; 455(7209):109–13. Epub 2008/08/01. doi: 10.1038/nature07159 nature07159 [pii]. PMID: 18668044; PubMed Central PMCID: PMC2610422.

67. White TA, Bartesaghi A, Borgnia MJ, Meyerson JR, de la Cruz MJ, Bess JW, et al. Molecular architectures of trimeric SIV and HIV-1 envelope glycoproteins on intact viruses: strain-dependent variation in quaternary structure. PLoS Pathog. 2010; 6(12):e1001249. doi: 10.1371/journal.ppat.1001249 PMID: 21203482; PubMed Central PMCID: PMC3009598.

68. Meyerson JR, White TA, Bliss D, Moran A, Bartesaghi A, Borgnia MJ, et al. Determination of molecular structures of HIV envelope glycoproteins using cryo-electron tomography and automated sub-tomogram averaging. J Vis Exp. 2011;(58:). doi: 10.3791/2770 PMID: 22158337; PubMed Central PMCID: PMC3304575.

69. Li C, Jin W, Du T, Wu B, Liu Y, Shattock RJ, et al. Binding of HIV-1 virions to alpha4beta 7 expressing cells and impact of antagonizing alpha4beta 7 on HIV-1 infection of primary CD4+ T cells. Virol Sin. 2014; 29(6):381–92. doi: 10.1007/s12250-014-3525-8 PMID: 25527342.